INTERNATIONAL JOURNAL OF
Telecommunications
AIR DEFENSE COLLEGE

# Comparative Evaluation and Optimal Selection Strategy for Enhanced PV String Performance under Irregular Shading Conditions: Application to PV Water Pumping System

**Dr. Ehab Mohamed Ali**

**Citation:** Mohamed Ali, E.; *Title. Inter. Jour. of Telecommunications, IJT'2025, Vol. 05, Issue 02, pp. 1-29, 2025.*

*Doi: 10.21608/ijt.2025.391168.1112*

**Editor-in-Chief:** Youssef Fayed.

Received: 01/06/2025.

Accepted date: 11/08/2025.
Published date: 11/08/2025.

**Publisher's Note: The International Journal of Telecommunications, IJT, stays neutral regarding jurisdictional claims in published maps and institutional affiliations.**



Electrical Engineering Department; Egyptian Air Defense College; Egyptian Military Academy; ehab.ali82@yahoo.com.
Correspondence: ehab.ali.7510m.adc@alexu.edu.eg.

**Abstract:** Photovoltaic (PV) systems are increasingly relied upon to power wide daily applications, especially since they are considered a clean and sustainable source of electricity generation. Moreover, they are considered a savior for remote areas that lack electricity grids. Despite their advantages, this system faces several challenges during operation, so it requires using various optimization algorithms to achieve optimal utilization and obtain the highest possible PV output power. One of the most serious challenges facing the PV system is operating under Irregular Shading Conditions (ISC). It significantly decreases the PV output power level. It also causes a complication in the shape of the PV power-voltage (P–V) curve, forming one Global Maximum Power (GMP) level among several Local ones. This study presents a comprehensive comparative evaluation of three modified control strategies to achieve the optimal controller selection for optimal PV system operation. These modified strategies are the Modified Cuckoo Search Algorithm (MCSA), the Modified Grey Wolf Optimizer (MGWO), and the Modified Particle Swarm Optimization (MPSO). They were studied and analyzed under irregular shading scenarios with gradually increasing complexity of the P–V curve for the PV system. The results reveal that all three modified algorithms outperform their conventional counterparts. A critical analysis was also provided to guide the most effective strategy for controlling PV systems in various applications, contributing to better decision-making during the design process to obtain maximum efficiency. By comparing the performance of the modified strategies, we concluded that MGWO is optimal at controlling PV system performance under various ambient conditions. It boasts the highest output efficiency and fastest tracking response. Furthermore, efficiency testing was conducted on a PV water pumping system that relies on an induction motor to drive the pump to confirm operational efficiency and provide final recommendations.

**Keywords:** Photovoltaic (PV); Irregular Shading Conditions (ISC); Photovoltaic Controller.

## 1. Introduction

The escalating global energy demand and the gradual exhaustion of fossil fuel reserves have underscored the urgent need to transition toward sustainable energy alternatives. Solar energy stands out among the various renewable sources due to its abundance, environmental compatibility, and long-term viability. In this context, photovoltaic (PV) systems have gained considerable attention as an effective means of harnessing solar radiation for electricity generation. While the upfront investment in PV technology can be substantial, these systems are characterized by durability, low operational costs, and broad geographic applicability. However, the performance of PV systems is highly dependent on environmental conditions, exhibiting irregular behavior in re-

sponse to fluctuations in solar irradiance and temperature. These variations become especially problematic in ISC, which can significantly diminish energy output. To mitigate these effects and maximize efficiency, sophisticated Maximum Power Point Tracking (MPPT) techniques are essential. With ongoing advancements in this field, solar energy continues to solidify its position as a reliable and sustainable alternative to traditional energy sources [1].

The efficiency of a PV system is primarily influenced by solar irradiance and ambient temperature, with optimal performance typically achieved at an irradiance level of approximately 1000 W/m² and a temperature of around 25°C [2]. The behavior of a PV system is commonly described by the PV output power-against-PV output voltage (P–V) curve, which under Regular Sun Irradiance (RSI) conditions exhibits a single Maximum Power Point (MPP). However, under ISC, the P–V curve becomes wavy and features multiple Local Maximum Power Peaks (LMPP), complicating the task of locating the Global Maximum Power Peak (GMPP) [3].

The DC-DC boost converter is a critical component in photovoltaic (PV) systems, responsible for adjusting the operating voltage of the PV modules to correspond to the maximum available output power. It operates by regulating the duty cycle, which defines the ratio of the switch's on-time to the total switching period. This ratio, expressed as a percentage or decimal, plays a key role in determining the Maximum Power Point (MPP) [4].

Traditional MPPT controllers such as the Modified Incremental Conductance (MIC) and Modified Perturb and Observe (MP&O) have introduced improvements over their classical counterparts; however, they still face significant limitations in accurately tracking the Global Maximum Power Point (GMPP), particularly under Irregular Shading Conditions. These algorithms often suffer from premature convergence to local maxima due to the multi-peak nature of the power–voltage (P–V) curve, resulting in suboptimal energy extraction and reduced overall system efficiency [5].

To address these challenges, recent research has increasingly shifted towards advanced and hybrid MPPT techniques that integrate artificial intelligence (AI) with traditional control strategies. These hybrid approaches aim to enhance tracking accuracy, convergence speed, and adaptability by combining the global search capability of AI-based algorithms with the simplicity and reliability of classical methods. A common hybridization strategy involves coupling metaheuristic optimization algorithms such as Particle Swarm Optimization (PSO), Genetic Algorithm (GA), Grey Wolf Optimizer (GWO), and Cuckoo Search Algorithm (CSA) with conventional MPPT techniques like Perturb and Observe (P&O) or Incremental Conductance (IC) [6-7]. For instance, PSO–P&O hybrids utilize PSO's exploratory strength to locate a near-optimal region, followed by P&O-based refinement to achieve faster convergence with reduced risk of local entrapment [8].

In addition, intelligent control paradigms such as neuro-fuzzy systems, which fuse Artificial Neural Networks (ANN) and Fuzzy Logic Controllers (FLC), have been proposed to tackle the nonlinear and uncertain behavior of PV systems. These approaches benefit from ANN's adaptive learning capabilities and FLC's rule-based reasoning, offering a self-tuning MPPT mechanism that performs reliably under dynamic environmental variations [9].

Moreover, ensemble-based hybrid techniques have been explored, wherein multiple optimization algorithms such as GA, PSO, Artificial Bee Colony (ABC) operate in parallel, and their outcomes are intelligently fused to determine the most suitable operating point. These methods enhance the robustness of the MPPT process, particularly under fast-varying irradiance or complex shading profiles. Despite their evident advantages in improving energy yield, such techniques introduce new challenges, including increased computational complexity, higher implementation costs, and the generation of transient power oscillations during the search process. These oscillations can prolong system stabilization time and potentially reduce tracking efficiency [10].

Consequently, ongoing research focuses on optimizing the trade-off between algorithmic sophistication and practical feasibility, with particular emphasis on reducing transient, enabling real-time embedded implementation, and ensuring consistent performance across diverse and uncertain operating conditions.

Ehab et al. added an effective technique to classical versions of CSA, GWO, and PSO by studying a detailed analysis of the P-V curve behaviors under the ISC. It enabled the prelimiting of algorithmic search spaces by banning voltage regions that do not contribute to maximum power output. Consequently, the modified versions are namely the Modified Particle Swarm Optimization (MPSO) [11], the Modified Grey Wolf Optimiza-

tion (MGWO) [12], and the Modified Cuckoo Search Algorithm (MCSA) [13]. Its targeted approach enhances algorithm efficiency by reducing transient oscillations and accelerating convergence speed.

This study presents a comparative analysis of the classical and modified versions of these algorithms, aiming to determine the most effective method for practical implementation. The algorithms have also been validated using a real-world case study involving a PV-powered water pumping system.

## 2. Materials and Methods

This section determines the simulation modeling and controlling of the solar PV system. It includes the PV module performance under RSI and its performance under ISC. It also discusses the PV System design, which includes the system controller (Max Power Point Tracking). This controller is estimated by different controller strategies based on classical and modified versions. A brief overview of each optimization algorithm will be provided to highlight their operational mechanisms and enhancements.

The modified Maximum Power Point Tracking (MPPT) algorithm iteratively refines the exploration area boundaries to enhance the performance of the presented algorithms. Initially, five evenly spread duty cycle samples are taken to cover the entire power-voltage (P-V) curve. The corresponding duty cycle, voltage, and power values for these samples are then stored in a matrix, sorted in descending order based on their operating voltage values for each iteration. The middle voltage value within this matrix is identified as a reference point, and its corresponding power value is considered the reference power for the current iteration. This reference power effectively divides the exploration area into two asymmetrical regions. The boundaries of each region are progressively narrowed towards the optimal solution in subsequent iterations, determined by the relationship between the reference power and other power values. When the reference power is the highest, the probability of finding the Global Maximum Power Point (GMPP) around that region increases, allowing the algorithm to disregard fewer probable areas and set new exploration limits. These improvements are derived from a comprehensive analysis of various P-V curve shapes under partial shading, which allows the algorithm to quickly establish new search boundaries at the end of each iteration, ensuring rapid convergence to the GMPP.

During the execution of the proposed algorithm, the two highest power values along with their corresponding duty cycles, denoted as D ($P_{max1}$) and D ($P_{max2}$), are retained. This strategy enhances the algorithm's effectiveness by preserving the regions of the search space that are more likely to contain the global optimum, thereby avoiding premature exclusion of promising areas. In each iteration, the algorithm updates the outside duty cycle sample with a new duty cycle value. This new value is positioned midway between the duty cycles corresponding to the two highest power points and is computed using the following equation.

$$D_{New} = D(P_{max2}) + \frac{D(P_{max1}) - D(P_{max2})}{2} \quad \text{(i)}$$

### *2.1. The Simulation Modeling of the Solar PV Module*

Using the MATLAB / Simulink program helps in conducting simulations with accurate results for the PV system and its operation. It plays an effective role and allows us to change the density of the sun's irradiation falling on the PV panels, modify the temperatures, and plot the output of the PV system. Consequently, it helps in studying the PV system behaviors for designing a suitable controller for its performance [14].

#### 2.1.1. PV under Regular Sun Irradiance (RSI)

The non-linear PV power versus voltage (P-V) curve illustrates all the operating points available for the PV system, ranging from zero voltage, which represents the short circuit condition, to the open circuit state, which contains the highest voltage value at which the PV system can be operated. Among these points, one operating point lets the PV system extract the maximum available power value. On the other hand, the shape of the PV current versus voltage (I-V) curve begins with the highest current value (short circuit case) and ends with a current value equal to zero (open circuit case), as shown in Figure 1 (a) [15].

#### 2.1.2. PV under Irregular Shading Conditions (ISC)

An irregularly shaded PV panel can be represented as comprising two groups of PV modules connected in series to form a PV string. Each group is paralleled by a bypass diode and subjected to varying levels of solar irradiance. Under conditions of irregular shading, the shaded cells absorb a portion of the electrical power

generated by the unshaded cells, effectively acting as electrical loads. This absorbed energy is dissipated as heat, which can result in the formation of hotspots that may ultimately damage the shaded cells [16].

To mitigate this issue, bypass diodes with opposite polarity are connected in parallel with each cell group. Under RSI conditions, these diodes remain in an open-circuit state. However, under irregular shading, they become forward bias and operate as short circuits, allowing the current from unshaded cells to bypass the shaded ones and thereby preventing damage. While this bypass mechanism protects the PV module, it also modifies the power output characteristics by introducing multiple local maxima in the power–voltage (P–V) curve as shown in Figure 1 (b) [17].

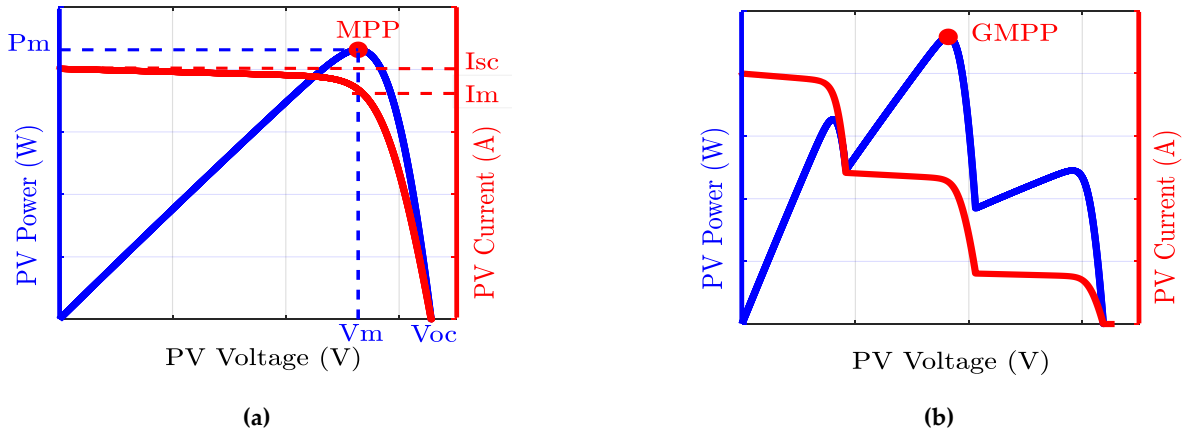


**Figure 1.** The Characteristics of PV Output Power against both the PV Output Voltage and PV Output Current (a) under Regular Sun Irradiance (RSI), (b) under Irregular Shading Conditions (ISC).

### *2.2. The Solar PV System Controller*

The Maximum Power Point Tracking (MPPT) controller for the PV system aims to achieve continuous operation at the highest achievable power output. A key element within this controller is the DC-DC boost converter, which functions based on a selected algorithm that generates and applies a controlled sequence of duty cycles. These duty cycles govern the switching behavior of the DC-DC boost converter, thereby modifying the effective impedance seen by the PV array. This adjustment process continues iteratively until the system's operating point coincides with the maximum power point, enabling optimal power extraction from the PV source.

In the following sections, a brief overview of each optimization algorithm will be provided to highlight their operational mechanisms and enhancements.

#### 2.2.1. The PV System Controller Based on CSA

The Cuckoo Search Algorithm (CSA), originally proposed by Yang and Deb in 2009, draws its inspiration from the brood parasitism exhibited by certain species of cuckoos. This optimization technique emulates the reproductive behavior of cuckoos, specifically their tendency to deposit eggs in the nests of other bird species. In addition, the algorithm employs Lévy flight-based stochastic movements to navigate the search space efficiently. CSA is widely acknowledged for its robust global optimization performance, ease of implementation, and strong capability to avoid entrapment in local minima characteristics that render it highly effective for real-time and complex optimization applications [18].

In the implementation of the CSA for PV systems controller, the nest positions representing candidate solutions are characterized by the duty cycle values (dc), which are input to the DC-DC boost converter. These duty cycles span a continuous range between 0 and 1, with number (n) of distinct values evaluated during each iteration. The *Le'vy* flight is employed to generate additional duty cycle samples $(dc_i^{(t+1)})$ using the following equation [19]:

$$dc_i^{(t+1)} = dc_i^{(t)} + k \times \left(\frac{u}{|v|^{1/\beta}}\right)(dc_{best} - dc_i) \qquad i = 1,2,\dots,n \qquad (1)$$

Where, in the notation ($dc_i^{(t+1)}$), the superscript (t) denotes the iteration number, while the subscript (i) refers to the index of the duty cycle. $k$ is represents the *Le'vy* scaling coefficient, the factor β=1.5, while the variables $v$ and $u$ are drawn from a normal distribution and are defined as follows:

$$u \approx N(0, \sigma_u^2) \quad , \quad v \approx N(0, \sigma_v^2) \tag{2}$$

Where

$$\sigma_v = 1 \quad , \quad \sigma_u = \left( \frac{\Gamma(1+\beta) \times \sin(\pi \times \beta/2)}{\Gamma((1+\beta)/2) \times \beta \times 2^{((\beta-1)/2)}} \right) \tag{3}$$

The variable $\Gamma$ is the integral gamma function.

The Pseudocode for using CSA in the PV system controller is as follows:

*Step 1:* Set the CSA strategy initial values as:

- The minimum and maximum limits for the duty cycles values are [$d_{min} = 0 \quad d_{max} = 1$].
- The first five nests position (duty cycles) vector are initialized as [0.1 0.3 0.5 0.7 0.9].
- The CSA discovery rate (pa = 0.25).

*Step 2:* Send each duty cycle to the boost converter and for each one calculate the fitness function (PV Output Power):

- Measured the PV output current $I_{pv}$ and PV output voltage $V_{pv}$.
- Calculate the PV output power $P_{pv} = I_{pv} \times V_{pv}$.
- Store the PV output power value.

*Step 3:* Identify the global optimal duty cycle ($d_{best}$) that corresponds to the iteration maximum output power ($P_{max}$).

*Step 4:* Identify the worst duty cycle ($d_{worst}$) that corresponds to the iteration minimum output power ($P_{min}$).

*Step 5:* If a random value is less than the discover rate (pa); replace ($d_{worst}$) with a new one using Levy flight equation.

- Measured the PV output current $I_{pv}$ and PV output Voltage $V_{pv}$.
- Calculate the PV output power $P_{pv} = I_{pv} \times V_{pv}$.
- Update the PV output power values by replacing the new power value with ($P_{min}$).
- Update the global optimal duty cycle ($d_{best}$).

*Step 6:* Generate the new nests (duty cycles) for the next iteration by using Levy flight equation.

*Step 7:* Repeat steps 2, 3, 4, and 5 for the present iteration.

*Step 8:* If all the duty cycles are equals and reached the MPP, stay on sending that optimal duty cycle to the boost converter; else repeat steps 6.

**Figure 2.** The Pseudocode for Using CSA in PV System Controller.

### 2.2.2. The PV System Controller Based on GWO Algorithm

The Gray Wolf Optimizer (GWO), proposed by Mirjalili et al. in 2014, is a nature-inspired metaheuristic algorithm that models the social hierarchy and cooperative hunting behaviors of gray wolves in their natural environment. The algorithm emulates the leadership structure of a wolf pack, consisting of alpha, beta, delta, and omega wolves, alongside their coordinated strategies for encircling, pursuing, and attacking prey. By replicating these social dynamics and adaptive hunting mechanisms, GWO achieves a balanced trade-off between exploration and exploitation within the search space. Its simplicity, robust convergence characteristics, and ability to avoid local optima contribute to its effectiveness, making it well-suited for solving complex real-time optimization problems [20].

The GWO algorithm is employed to update the Wolves positions (duty cycles) samples ($dc_i^{(t+1)}$) based on the equation 4. The position of the prey (Maximum PV Output Power) can be expressed by ($X_P$). Also, the position of the Grey Wolfe (duty cycle) can be expressed by ($X$).

$$\overrightarrow{dc_{\iota}^{(t+1)}} = \left| \overrightarrow{X_P} - \overrightarrow{A} \cdot \overrightarrow{D} \right| \quad (4)$$

Where;

$$\overrightarrow{A} = 2 \times a \times r_1 - a \quad , \quad \overrightarrow{D} = \left| \overrightarrow{C} \cdot \overrightarrow{X_P} - \overrightarrow{X}(t) \right| \quad (5)$$

Also;

$$\overrightarrow{C} = 2 \times r_2 \quad (6)$$

Where ( $r_1$ , $r_2$ ) are random values within the range [0,1], while (a) is a control parameter that linearly decreases from 2 to 0 over the course of iterations. This decreasing behavior models the transition from exploration to exploitation where higher values of (a) encourage exploration of the search space, and as (a) approaches zero, the wolves converge on the prey (the algorithm catch and track the maximum available PV output power), simulating the final stage of the hunt at zero distance [21].

The Pseudocode for using GWO in the PV system controller is as follows:

*Step 1:* Set the GWO strategy initial values as:

- The minimum and maximum limits for the duty cycles values are [$d_{min} = 0 \quad d_{max} = 1$].
- The first five Wolves (duty cycles) vector are initialized as [0.1 0.3 0.5 0.7 0.9].

*Step 2:* Send each duty cycle to the boost converter and for each one calculate the fitness function (PV Output Power):

- Measured the PV output current $I_{pv}$ and PV output voltage $V_{pv}$.
- Calculate the PV output power $P_{pv} = I_{pv} \times V_{pv}$.
- Store the PV output power value.

*Step 3:* Identify the Alpha wolf that corresponds to the highest output power value. Identify the Beta wolf that corresponds to the second highest output power value. Identify the Delta wolves that corresponds to the third, fourth, and fifth output power values.

*Step 4:* Update the Wolves position (duty cycles) by using equation 4.

*Step 5:* Repeat steps 2 and 3 for the present iteration.

*Step 6:* If all the Wolves position (duty cycles) are equals and reached the MPP, stay on sending that duty cycle to the boost converter; else repeat steps 4.

**Figure 3.** The Pseudocode for Using GWO in PV System Controller.

### 2.2.3. The PV System Controller Based on PSO Algorithm

Particle Swarm Optimization (PSO), first introduced by Kennedy and Eberhart in 1995, is a nature-inspired metaheuristic algorithm that draws inspiration from the collective social behaviors exhibited by flocks of birds and schools of fish. The algorithm models a swarm of particles representing candidate solutions, which iteratively update their positions in the search space by leveraging both individual experiences and the shared knowledge within the swarm. This dynamic interaction facilitates an effective balance between exploration and exploitation, enabling PSO to efficiently navigate complex optimization landscapes. Renowned for its conceptual elegance, rapid convergence properties, and resilience against premature convergence to local optima, PSO has been extensively applied to solve a diverse array of challenging real-world optimization problems [22].

In the implementation of the PSO for PV systems controller, the algorithm's parameters are fine-tuned to align with the characteristics of the PV system. These parameters include the swarm acceleration coefficient ($\alpha$), set between 2 and 2.5, the inertia weight ($\theta$), fixed at 0.5, and the self-acceleration coefficient ($\beta$), set between 1.5 and 2. At each iteration, the velocity $v_i^{t+1}$ and position $dc_i^{t+1}$ of each particle are updated using equations (7) and (8), respectively [23].

$$v_i^{t+1} = \theta v_i^t + \alpha\epsilon_1(dc_{Gbest} - dc_i^t) + \beta\epsilon_2(dc_{i\_best} - dc_i^t) \quad (7)$$

$$dc_i^{t+1} = dc_i^t + v_i^{t+1} \quad (8)$$

The Pseudocode for using PSO in the PV system controller is as follows:

*Step 1:* Set the PSO strategy initial values as:
- The minimum and maximum limits for the duty cycles values are [$d_{min} = 0 \quad d_{max} = 1$].
- The first five particles (duty cycles) vector are initialized as [0.1 0.3 0.5 0.7 0.9].
- Let the personal best position for each particle is zero.

*Step 2:* Send each duty cycle to the boost converter and for each one calculate the fitness function (PV Output Power):
- Measured the PV output current $I_{pv}$ and PV output voltage $V_{pv}$.
- Calculate the PV output power $P_{pv} = I_{pv} \times V_{pv}$.
- Store the PV output power value.

*Step 3:* Identify the global best position that corresponds to the obtained maximum output power ($P_{max}$).

*Step 4:* For each particle (duty cycle), If its corresponds output power is greater than its personal best position, update the particle personal best position.

*Step 5:* If the output power for any particle is greater than the global best position, update the global best position.

*Step 6:* Update the particles position and velocity to obtain the newest duty cycles by using equation 8.

*Step 7:* Repeat steps 2, 3, 4 and 5 for the present iteration.

*Step 8:* If all the particles position (duty cycles) are equals and reached the MPP, stay on sending that duty cycle to the boost converter; else repeat steps 6.

**Figure 4.** The Pseudocode for Using PSO in PV System Controller.

### 2.2.4. The PV System Controller Based on MCSA

The efficiency of the classical CSA has been significantly enhanced through the incorporation of an auxiliary sub-strategy. This sub-strategy, implemented as a dedicated software module, is responsible for extracting key measurement data from the CSA, followed by systematic data processing, organization, and storing the iterations' data. The processed information enables the identification of a high-potential region on the P–V characteristic curve, where the likelihood of locating the maximum available output power is substantially increased. These refined boundaries are subsequently communicated back to the primary CSA, thereby guiding and constraining the search process within more promising solution spaces and improving overall convergence performance [13].

The flowchart for using MCSA in the PV system controller is as follows:

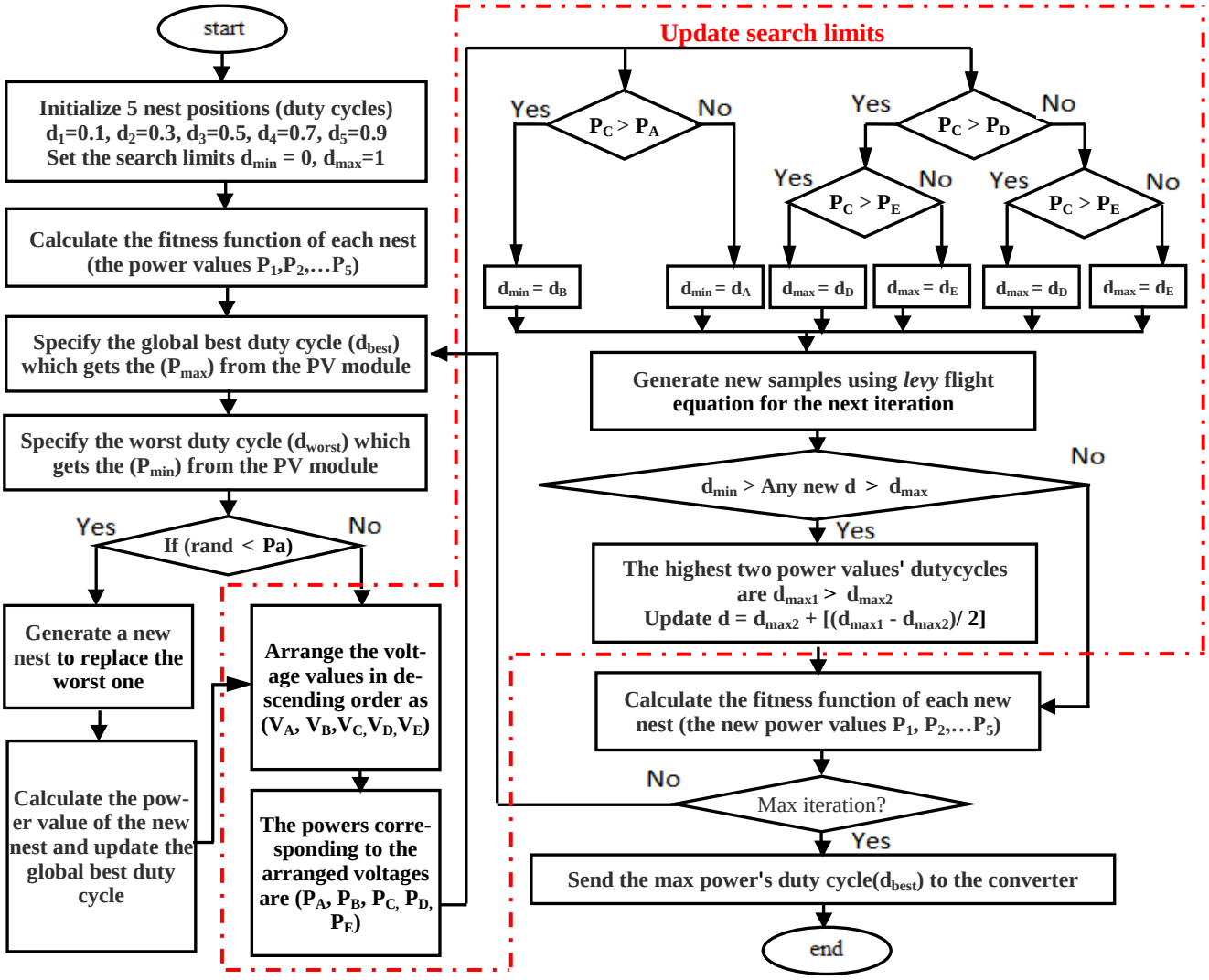


**Figure 5.** The Flowchart for Using MCSA in PV System Controller.

The Pseudocode for using MCSA in the PV system controller is as follows:

*Step 1:* Set the MCSA strategy initial values as:

- The minimum and maximum limits for the duty cycles values are $[d_{min} = 0 \quad d_{max} = 1]$.
- The first five nests position (duty cycles) vector are initialized as [0.1 0.3 0.5 0.7 0.9].
- The CSA discovery rate (pa = 0.25).

*Step 2:* Send each duty cycle to the boost converter and for each one calculate the fitness function (PV Output Power):

- Measured the PV output current $I_{pv}$ and PV output Voltage $V_{pv}$.
- Calculate the PV output power $P_{pv} = I_{pv} \times V_{pv}$.
- Store the iteration values in a vector matrix as

$$\begin{bmatrix} \text{Iteration number} \# \# \# & \text{nest number} \# & I_{pv} & V_{pv} & P_{pv} & d_{pv} \\ \vdots \# & \vdots \# & \vdots & \vdots & \vdots & \vdots \end{bmatrix}$$

*Step 3:* Identify the global optimal duty cycle ($d_{best}$) that corresponds to the iteration maximum output power ($P_{max}$).

*Step 4:* Identify the worst duty cycle ($d_{worst}$) that corresponds to the iteration minimum output power ($P_{min}$).

*Step 5:* If a random value is less than the discover rate (pa); replace ($d_{worst}$) with a new one using Levy flight equation.

- Measured the PV output current $I_{pv}$ and PV output Voltage $V_{pv}$.
- Calculate the PV output power $P_{pv} = I_{pv} \times V_{pv}$.
- Update the PV output power values by replacing the new power value with ($P_{min}$).
- Update the global optimal duty cycle ($d_{best}$).

*Step 6:* After each iteration update the limits of the search area on P-V curve by;

- Sort in descending order the iteration matrix rows according to the output PV voltage ($V_{pv}$).
- Rename the arranged PV voltage values as: $(V_A < V_B < V_C < V_D < V_E)$.
- Rename the PV power values associate to the arranged voltages to be: $(P_A,\ P_B,\ P_C,\ P_D,\ P_E)$.
- Rename the duty cycles values associate to the arranged voltages to be: $(d_A,\ d_B,\ d_C,\ d_D,\ d_E)$.
- Update the new limits $(d_{max} \& d_{min})$ on the P-V curve for the next iteration search process as:

if $P_C > P_A$, set $d_{min} = d_B$; else set $d_{min} = d_A$.

if $P_C > P_E$, set $d_{max} = d_D$; else set $d_{max} = d_E$.

*Step 7:* Identify the highest stored power values $(P_{max_1} \& P_{max_2})$ and its associated duty cycles values $(d_{Pmax_1} \& d_{Pmax_2})$.

*Step 8:* The CSA start to generate the new nests (duty cycles) for the next iteration by using Levy flight equation then:

- check each new duty cycle as:

if $d_{new_i} > d_{max}$, set $d_{new_i} = d_{Pmax_2} + [(d_{Pmax_1} - d_{Pmax_2})/2]$.

if $d_{new_i} < d_{min}$, set $d_{new_i} = d_{Pmax_2} + [(d_{Pmax_1} - d_{Pmax_2})/2]$.

*Step 9:* Repeat steps 2, 3, 4, and 5 for the present iteration.

*Step 10:* If all the duty cycles are equals and reached the MPP, stay on sending that optimal duty cycle to the boost converter; else repeat steps 6.

**Figure 6.** The Pseudocode for Using MCSA in PV System Controller.

2.2.5. The PV System Controller Based on MGWO Algorithm

The same previous software sub-strategy is added to the classical GWO algorithm to enhance the algorithm's performance. The classical algorithm has interacted with it in an excellent way to narrow the search area after each iteration [12].

The flowchart for using MGWO in the PV system controller is as follows:

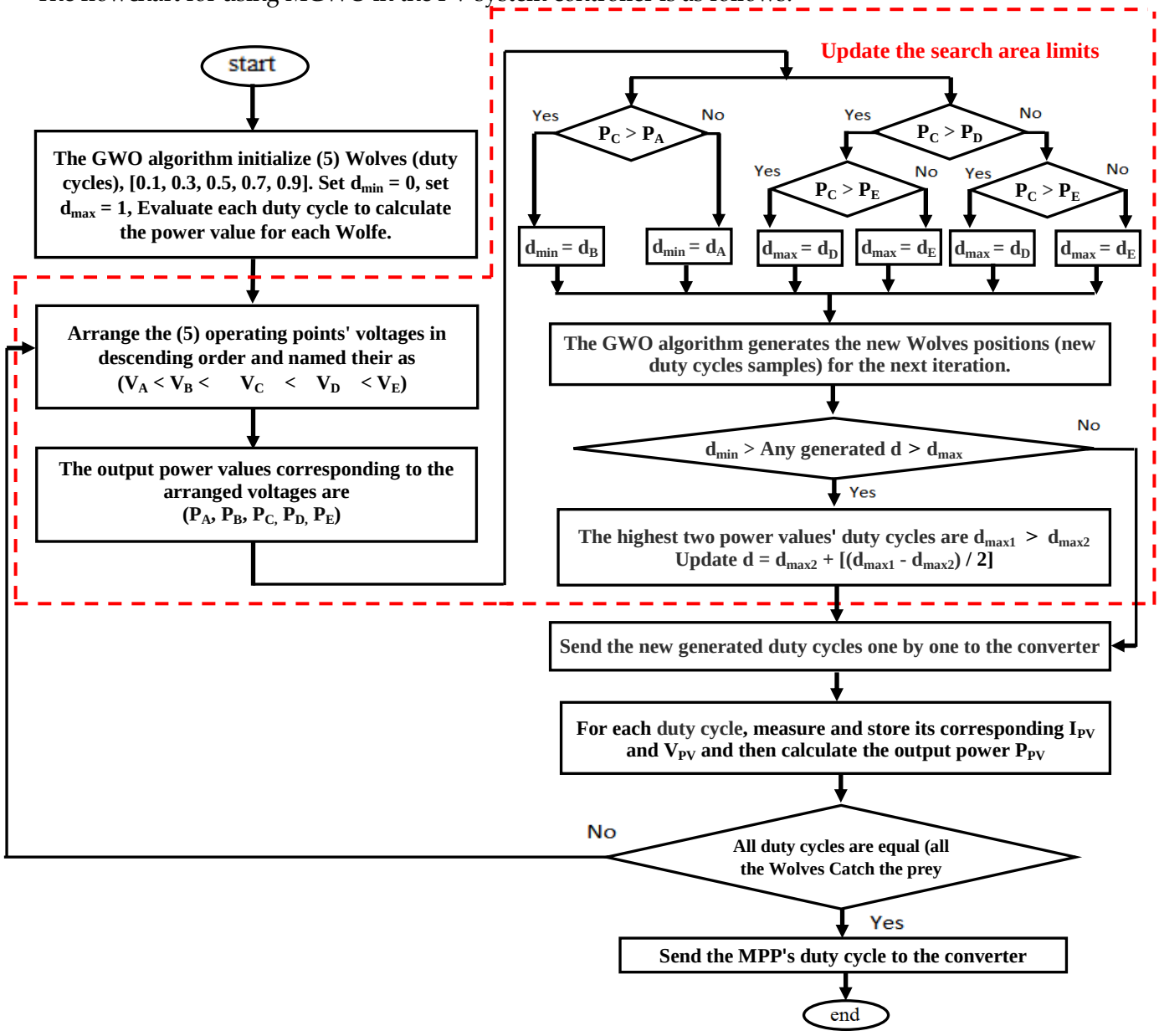


**Figure 7.** The Flowchart for Using MGWO in PV System Controller.

The Pseudocode for using MGWO in the PV system controller is as follows:

*Step 1:* Set the MGWO strategy initial values as:

- The minimum and maximum limits for the duty cycles values are $[d_{min} = 0 \quad d_{max} = 1]$.
- The first five Wolves (duty cycles) vector are initialized as [0.1 0.3 0.5 0.7 0.9].

*Step 2:* Send each duty cycle to the boost converter and for each one calculate the fitness function (PV Output Power):

- Measured the PV output current $I_{pv}$ and PV output voltage $V_{pv}$.
- Calculate the PV output power $P_{pv} = I_{pv} \times V_{pv}$.
- Store the iteration values in a vector matrix as

$$\begin{bmatrix} \text{Iteration number} \# \# \# & \text{nest number} \# & I_{pv} & V_{pv} & P_{pv} & d_{pv} \\ \vdots \# & \vdots \# & \vdots & \vdots & \vdots & \vdots \end{bmatrix}$$

*Step 3:* Identify the Alpha wolf that corresponds to the highest output power value. Identify the Beta wolf that corresponds to the second highest output power value. Identify the Delta wolves that corresponds to the third, fourth, and fifth output power values.

*Step 4:* After each iteration update the limits of the search area on P-V curve by;

- Sort in descending order the iteration matrix rows according to the output PV voltage ($V_{pv}$).
- Rename the arranged PV voltage values as: $(V_A < V_B < V_C < V_D < V_E)$.
- Rename the PV power values associate to the arranged voltages to be: $(P_A,\ P_B,\ P_C,\ P_D,\ P_E)$.
- Rename the duty cycles values associate to the arranged voltages to be: $(d_A,\ d_B,\ d_C,\ d_D,\ d_E)$.
- Update the new limits $(d_{max} \& d_{min})$ on the P-V curve for the next iteration search process as:

if $P_C > P_A$, set $d_{min} = d_B$; else set $d_{min} = d_A$.

if $P_C > P_E$, set $d_{max} = d_D$; else set $d_{max} = d_E$.

*Step 5:* Identify the highest stored power values $(P_{max_1} \& P_{max_2})$ and its associated duty cycles values $(d_{Pmax_1} \& d_{Pmax_2})$.

*Step 6:* The GWO start to update the Wolves positions (duty cycles) for the next iteration by using equation 4 then:

- check each new duty cycle as:

if $d_{new_i} > d_{max}$, set $d_{new_i} = d_{Pmax_2} + [(d_{Pmax_1} - d_{Pmax_2})/2]$.

if $d_{new_i} < d_{min}$, set $d_{new_i} = d_{Pmax_2} + [(d_{Pmax_1} - d_{Pmax_2})/2]$.

*Step 7:* Repeat steps 2 and 3 for the present iteration.

*Step 8:* If all the Wolves position (duty cycles) are equals and reached the MPP, stay on sending that duty cycle to the boost converter; else repeat steps 4, 5, 6, and 7.

**Figure 8.** The Pseudocode for Using MGWO in PV System Controller.

### 2.2.6. The PV System Controller Based on MPSO Algorithm

The previously described software-based sub-strategy has also been integrated into the classical PSO algorithm to enhance its performance. The classical PSO demonstrated effective synergy with the sub-strategy, utilizing it to progressively refine and constrain the search space following each iteration [24].

The flowchart for using MPSO in the PV system controller is as follows:

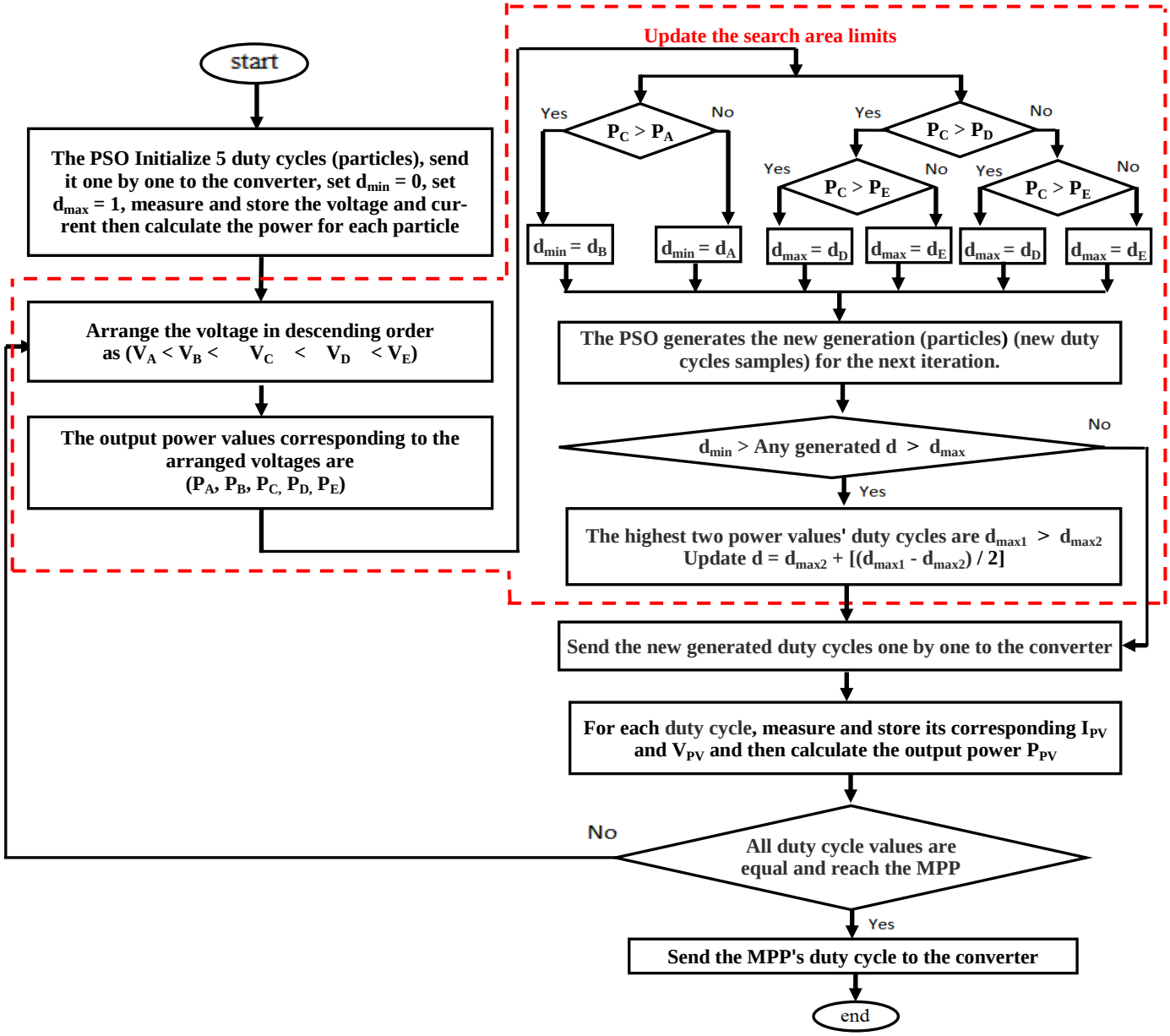


**Figure 9.** The Flowchart for Using MPSO in PV System Controller.

The Pseudocode for using MPSO in the PV system controller is as follows:

*Step 1:* Set the MPSO strategy initial values as:

- The minimum and maximum limits for the duty cycles values are $[d_{min} = 0 \quad d_{max} = 1]$.
- The first five particles (duty cycles) vector are initialized as [0.1 0.3 0.5 0.7 0.9].
- Let the personal best position for each particle is zero.

*Step 2:* Send each duty cycle to the boost converter and for each one calculate the fitness function (PV Output Power):

- Measured the PV output current $I_{pv}$ and PV output voltage $V_{pv}$.
- Calculate the PV output power $P_{pv} = I_{pv} \times V_{pv}$.
- Store the iteration values in a vector matrix as

$$\begin{bmatrix} \text{Iteration number} & \text{nest number} & I_{pv} & V_{pv} & P_{pv} & d_{pv} \\ \vdots & \vdots & \vdots & \vdots & \vdots & \end{bmatrix}$$

*Step 3:* Identify the global best position that corresponds to the iteration maximum output power ($P_{max}$).

*Step 4:* For each particle (duty cycle), If its corresponds output power is greater than its personal best position, update the particle personal best position.

*Step 5:* If the output power for any particle is greater than the global best position, update the global best position.

*Step 6:* After each iteration update the limits of the search area on P-V curve by;

- Sort in descending order the iteration matrix rows according to the output PV voltage ($V_{pv}$).
- Rename the arranged PV voltage values as: $(V_A < V_B < V_C < V_D < V_E)$.
- Rename the PV power values associate to the arranged voltages to be: $(P_A,\ P_B,\ P_C,\ P_D,\ P_E)$.
- Rename the duty cycles values associate to the arranged voltages to be: $(d_A,\ d_B,\ d_C,\ d_D,\ d_E)$.
- Update the new limits $(d_{max} \& d_{min})$ on the P-V curve for the next iteration search process as:

if $P_C > P_A$, set $d_{min} = d_B$; else set $d_{min} = d_A$.

if $P_C > P_E$, set $d_{max} = d_D$; else set $d_{max} = d_E$.

*Step 7:* Identify the highest stored power values $(P_{max_1} \& P_{max_2})$ and its associated duty cycles values $(d_{Pmax_1} \& d_{Pmax_2})$.

*Step 8:* The PSO start to update the particles position and velocity (duty cycles) for the next iteration by using equation 8 then:

- check each new duty cycle as:

if $d_{new_i} > d_{max}$, set $d_{new_i} = d_{Pmax_2} + [(d_{Pmax_1} - d_{Pmax_2})/2]$.

if $d_{new_i} < d_{min}$, set $d_{new_i} = d_{Pmax_2} + [(d_{Pmax_1} - d_{Pmax_2})/2]$.

*Step 9:* Repeat steps 2, 3, 4 and 5 for the present iteration.

*Step 10:* If all the particles position (duty cycles) are equals and reached the MPP, stay on sending that duty cycle to the boost converter; else repeat steps 6, 7, and 8.

**Figure 10.** The Pseudocode for Using MPSO in PV System Controller.

## 3. Results and Discussion

### *3.1. The Different Simulated PV Systems*

The PV system simulated at four different shapes to imitate PV strings subjected to RSI or ISC.

The first PV string (pattern-1), consists of two PV modules each of them exposure to uniform sun light density of $1000\ W/m^2$ and operates at the surrounding temperature of $25^0$. This pattern mimics a PV string operates at RSI. In this case, the PV String output has a maximum available power of value 260W. This maxi-

mum power can be obtained when the PV string operates at voltage of 35.5V, and current of 7.3A as shown in the PV system characteristics' curves of Figure 11 (a, b).

The second PV string (pattern-2), consists of two PV modules each of them operates at the surrounding temperature of $25^0$ and exposure to non-uniform sun light of $1000\,W/m^2$ and $600\,W/m^2$ respectively. This pattern mimics a PV string that operates at ISC. In this case, the PV String output has a global maximum power of value 170W. This global maximum power can be obtained when the PV string operates at voltage of 37V, and current of 4.6A as shown in the PV system characteristics' curves of Figure 11 (c, d).

The third PV string (pattern-3), consists of three PV modules each of them operates at the air temperature of $25^0$ and exposure to non-uniform sun light of $1000\,W/m^2$, $600\,W/m^2$ and $200\,W/m^2$ respectively. This pattern mimics a PV string operates at complex ISC. In this case, the PV String output has a global maximum power of value 165W. This global maximum power can be obtained when the PV string operates at voltage of 36.5V, and current of 4.5A as shown in the PV system characteristics' curves of Figure 11 (e, f).

The fourth PV string (pattern-4), consist of four PV modules each of them operates at the environmental temperature of $25^0$ and exposure to non-uniform sun light of $1000\,W/m^2$, $700\,W/m^2$, $500\,W/m^2$ and $300\,W/m^2$ respectively. This pattern mimics a PV string that operates at more complex ISC. In this case, the PV String output has a global maximum power of value 215W. This global maximum power can be obtained when the PV string operates at voltage of 56V, and current of 3.8A as shown in the PV system characteristics' curves of Figure 11 (g, h).

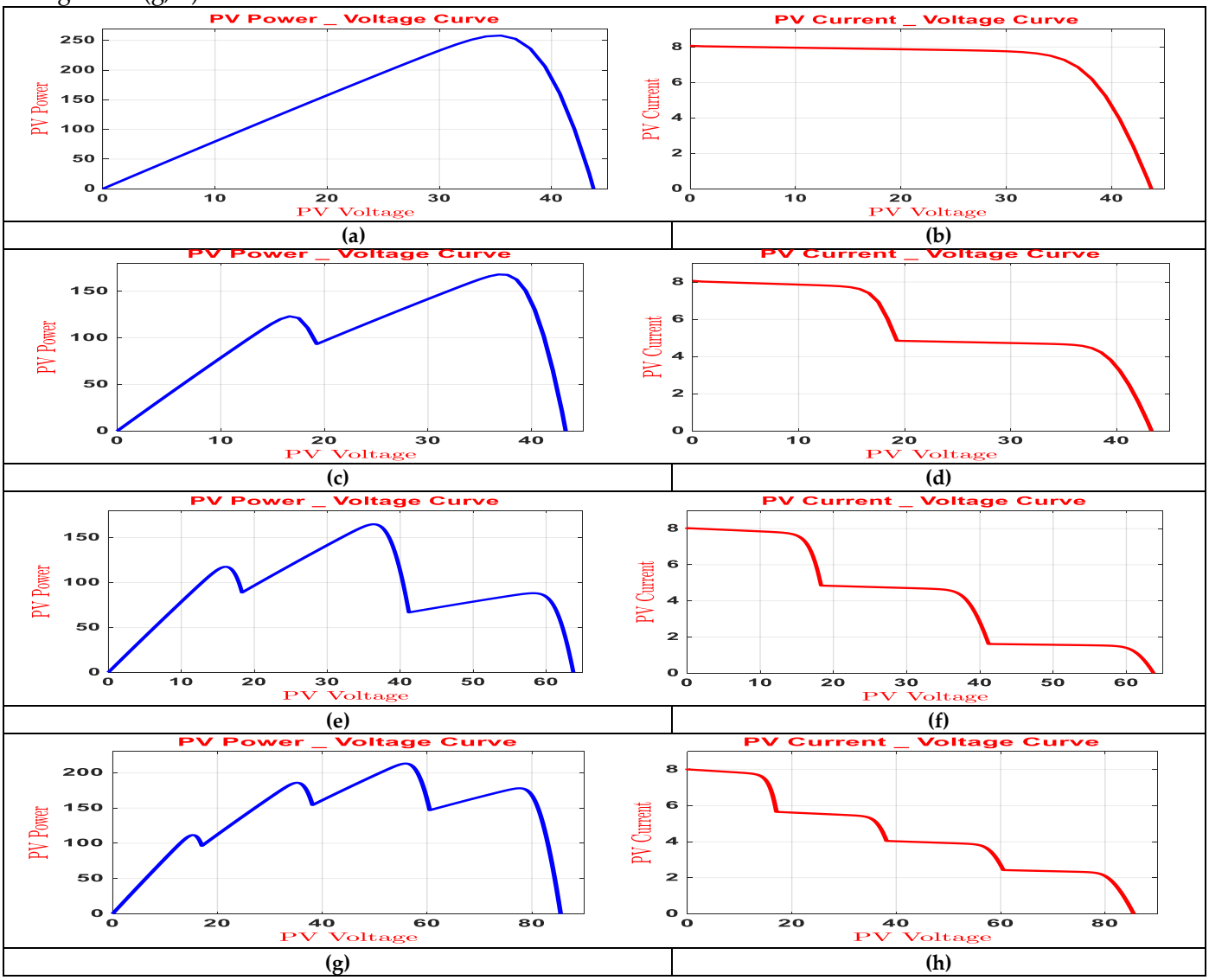


**Figure 11.** Different Shapes of PV System Characteristics.

The four-pattern data can be summarized in Table 1.

**Table 1.** The Four-PV Pattern Data.

| PV String | Number of PV Modules | Irradiance at each Module ($W/m^2$) | Surrounding Temperature | Maximum Power Point | | |
|---|---|---|---|---|---|---|
| | | | | Value | Voltage | Current |
| Pattern-1 | 2 | [1000 1000] | $25^0$ | 260W | 35.5V | 7.3A |
| Pattern-2 | 2 | [1000 600] | $25^0$ | 170W | 37V | 4.6A |
| Pattern-3 | 3 | [1000 600 200] | $25^0$ | 165W | 36.5V | 4.5A |
| Pattern-4 | 4 | [1000 700 500 300] | $25^0$ | 215W | 56V | 3.8A |

*3.2. Evaluating the First PV System Pattern (Pattern-1) by Different Algorithms*

The first evaluation is based on tracking the maximum available output power when the PV system controller is based on the Classical CSA (CCSA). In this case, the PV system output power versus the convergence speed curve is shown in Figure 12 (a). It can be seen that the CCSA succeeds in letting the PV system deliver the maximum power it could extract, which is equal to 254.2W. The convergence speed takes 0.8s. During the convergence, the transient state has medium oscillations, and the steady state has a high stable and flat output. The pattern-1 output efficiency can be calculated as 97.77%.

The second evaluation is to monitor the maximum available output power tracking for the PV system by using the Classical GWO (CGWO). Figure 12 (c) illustrates the relationship between the PV system's output power and its convergence speed. The results indicate that the CGWO effectively enabled the PV system to deliver its maximum extractable power of 254.9W within a convergence time of 0.74s. During this convergence, the system exhibited high oscillations before reaching a high stable and consistent steady-state output. The calculated pattern-1 output efficiency was 98.04%.

The third evaluation tracked the maximum available output power of the PV system depending on the Classical PSO (CPSO). Figure 12 (e) shows how the PV system's power output and convergence speed were related in this evaluation. The figure reveals that the CPSO, successfully allowed the PV system to track its maximum power of 254.7W in a long time of 1.53s. During this convergence time, the system displayed high oscillations before settling into a minor oscillations output. The determined pattern-1 output efficiency was 97.96%.

The fourth evaluation is to monitor the maximum available output power tracking for the PV system by using the Modified CSA (MCSA). Figure 12 (b) illustrates the correlation between the PV system's output power and its rate of convergence during this assessment. The results indicated that the MCSA effectively enabled the PV system to track the maximum available output power of 254.1W within 0.49s. Throughout this convergence, the system exhibited significant fluctuations before establishing a steady and high stable output. The calculated efficiency of the pattern-1's output was 97.73%

The fifth evaluation tracked the maximum available output power of the PV system depending on the Modified GWO (MGWO). Figure 12 (d) shows how the PV system's power output and convergence speed were related in this evaluation. The figure reveals that the MGWO successfully allowed the PV system to track its maximum power of 257.6W in a short time of 0.17s. Notably, the system's output fluctuated slightly before stabilizing during this convergence period. The determined output efficiency of the pattern-1 was 99.08%.

The sixth evaluation's results indicated that the PV system can use the Modified PSO (MPSO) to reach the maximum available output power of 257.1W in 0.29s. As depicted in Figure 12 (f), the PV system's output power was linked to its convergence speed by a slight fluctuating output before settling with high stable during the steady state. The calculated efficiency of the pattern-1's output was 98.88%.

*3.3. Evaluating the Second PV System Pattern (Pattern-2) by Different Algorithms*

The first evaluation is to monitor the global maximum available output power tracking for the PV system by using the Classical CSA (CCSA). Figure 13 (a) illustrates the relationship between the PV system's output power and its convergence speed. The results indicate that the CCSA effectively enabled the PV system to deliver its global maximum extractable power of 168.27W within a convergence time of 0.98s. During this convergence, the system exhibited medium oscillations before reaching a high stable and consistent steady-state output. The calculated pattern-2 output efficiency was 98.98%.

The second evaluation is based on tracking the global maximum available output power when the PV system controller is based on the Classical GWO (CGWO). In this case, the PV system output power versus the convergence speed curve is shown in Figure 13 (c). It can be seen that, the CGWO succeeds in letting the PV system deliver the global maximum power it could extract, which is equal to 168.67W. The convergence speed takes 0.73s. During the convergence, the transient state has high oscillations, and the steady state has a high stable and flat output. The pattern-2 output efficiency can be calculated as 99.22%.

The third evaluation tracked the global maximum available output power of the PV system depending on the Classical PSO (CPSO). Figure 13 (e) shows how the PV system's power output and convergence speed were related in this evaluation. The figure reveals that the CPSO, successfully allowed the PV system to track its global maximum power of 168.2W in a long time of 1.89s. During this convergence time, the system displayed medium oscillations before settling into a minor oscillations output. The determined pattern-2 output efficiency was 98.94%.

The fourth evaluation is to monitor the global maximum available output power tracking for the PV system by using the Modified CSA (MCSA). Figure 13 (b) illustrates the correlation between the PV system's output power and its rate of convergence during this assessment. The results indicated that the MCSA effectively enabled the PV system to track the global maximum available output power of 166.68W within 0.25s. Throughout this convergence, the system exhibited significant fluctuations before establishing a steady and high stable output. The calculated efficiency of the pattern-2's output was 98.05%

The fifth evaluation tracked the global maximum available output power of the PV system depending on the Modified GWO (MGWO). Figure 13 (d) shows how the PV system's power output and convergence speed were related in this evaluation. The figure reveals that the MGWO successfully allowed the PV system to track its maximum power of 168.6W in a short time of 0.17s. Notably, the system's output fluctuated slightly before reaching high stabilizing during this convergence period. The determined output efficiency of the pattern-2 was 99.18%.

The sixth evaluation's results indicated that the PV system can use the Modified PSO (MPSO) to reach the global maximum available output power of 168.53W in 0.35s. As depicted in Figure 13 (f), the PV system's output power was linked to its convergence speed by a slight fluctuating output before settling with high stable during the steady state. The calculated efficiency of the pattern-2's output was 99.14%.

*3.4. Evaluating the Third PV System Pattern (Pattern-3) by Different Algorithms*

The first evaluation tracked the global maximum available output power of the PV system depending on the Classical CSA (CCSA). Figure 14 (a) shows how the PV system's power output and convergence speed were related in this evaluation. The figure reveals that the CCSA, successfully allowed the PV system to track its global maximum power of 163.34W in a time of 0.79s. During this convergence time, the system displayed medium oscillations before settling into a high stable output. The determined pattern-3 output efficiency was 98.99%.

The second evaluation is to monitor the global maximum available output power tracking for the PV system by using the Classical GWO (CGWO). Figure 14 (c) illustrates the relationship between the PV system's output power and its convergence speed. The results indicate that the CGWO effectively enabled the PV system to deliver its global maximum extractable power of 164.49W within a convergence time of 0.73s. During this convergence, the system exhibited medium oscillations before reaching a high stable and consistent steady-state output. The calculated pattern-3 output efficiency was 99.69%.

The third evaluation is based on tracking the global maximum available output power when the PV system controller is based on the Classical PSO (CPSO). In this case, the PV system output power versus the conver-

gence speed curve is shown in Figure 14 (e). It can be seen that, the CPSO succeeds in letting the PV system deliver the global maximum power it could extract, which is equal to 163.87W. The convergence speed takes long time of 1.88s. During the convergence, the transient state has medium oscillations, and the steady state has a minor oscillations output. The pattern-3 output efficiency can be calculated as 99.32%.

The fourth evaluation is to monitor the global maximum available output power tracking for the PV system by using the Modified CSA (MCSA). Figure 14 (b) illustrates the correlation between the PV system's output power and its rate of convergence during this assessment. The results indicated that the MCSA effectively enabled the PV system to track the global maximum available output power of 163.9W within 0.28s. Throughout this convergence, the system exhibited significant fluctuations before establishing a steady and high stable output. The calculated efficiency of the pattern-3's output was 99.33%

The fifth evaluation tracked the global maximum available output power of the PV system depending on the Modified GWO (MGWO). Figure 14 (d) shows how the PV system's power output and convergence speed were related in this evaluation. The figure reveals that the MGWO successfully allowed the PV system to track its maximum power of 164.8W in a short time of 0.15s. Notably, the system's output fluctuated slightly before reaching high stabilizing during this convergence period. The determined output efficiency of the pattern-3 was 99.88%.

The sixth evaluation's results indicated that the PV system can use the Modified PSO (MPSO) to reach the global maximum available output power of 164.6W in 0.35s. As depicted in Figure 14 (f), the PV system's output power was linked to its convergence speed by a slight fluctuating output before settling with high stable during the steady state. The calculated efficiency of the pattern-3's output was 99.76%.

### *3.5. Evaluating the Fourth PV System Pattern (Pattern-4) by Different Algorithms*

The first evaluation is based on tracking the maximum available output power when the PV system controller is based on the Classical CSA (CCSA). In this case, the PV system output power versus the convergence speed curve is shown in Figure 15 (a). It can be seen that the CCSA succeeds in letting the PV system deliver the maximum power it could extract, which is equal to 207.1W. The convergence speed takes 0.74s. During the convergence, the transient state has medium oscillations, and the steady state has a high stable and flat output. The pattern-4 output efficiency can be calculated as 96.33%.

The second evaluation is to monitor the maximum available output power tracking for the PV system by using the Classical GWO (CGWO). Figure 15 (c) illustrates the relationship between the PV system's output power and its convergence speed. The results indicate that the CGWO effectively enabled the PV system to deliver its maximum extractable power of 210.26W within a convergence time of 0.72s. During this convergence, the system exhibited medium oscillations before reaching a high stable and consistent steady-state output. The calculated pattern-4 output efficiency was 97.80%.

The third evaluation tracked the maximum available output power of the PV system depending on the Classical PSO (CPSO). Figure 15 (e) shows how the PV system's power output and convergence speed were related in this evaluation. The figure reveals that the CPSO, successfully allowed the PV system to track its maximum power of 209.1W in a long time of 1.52s. During this convergence time, the system displayed medium oscillations before settling into a minor oscillations output. The determined pattern-4 output efficiency was 97.26%.

The fourth evaluation is to monitor the maximum available output power tracking for the PV system by using the Modified CSA (MCSA). Figure 15 (b) illustrates the correlation between the PV system's output power and its rate of convergence during this assessment. The results indicated that the MCSA effectively enabled the PV system to track the maximum available output power of 205.8W within 0.25s. Throughout this convergence, the system exhibited significant fluctuations before establishing a steady and high stable output. The calculated efficiency of the pattern-4's output was 95.72%

The fifth evaluation tracked the maximum available output power of the PV system depending on the Modified GWO (MGWO). Figure 15 (d) shows how the PV system's power output and convergence speed were related in this evaluation. The figure reveals that the MGWO successfully allowed the PV system to track its maximum power of 210.19W in a short time of 0.23s. Notably, the system's output fluctuated slightly before stabilizing during this convergence period. The determined output efficiency of the pattern-4 was 97.76%.

The sixth evaluation's results indicated that the PV system can use the Modified PSO (MPSO) to reach the maximum available output power of 202.37W in 0.26s. As depicted in Figure 15 (f), the PV system's output

power was linked to its convergence speed by a slight fluctuating output before settling with high stable during the steady state. The calculated efficiency of the pattern-4's output was 94.13%.

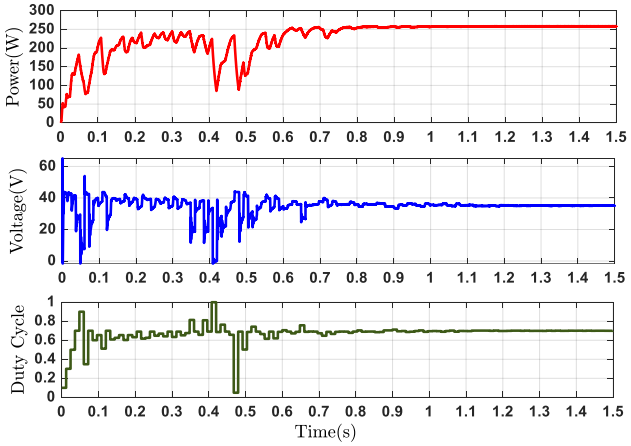


**(a) Classical CSA**

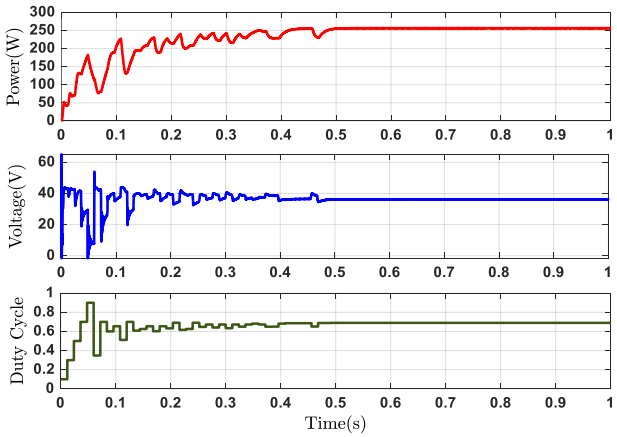


**(b) Modified CSA**

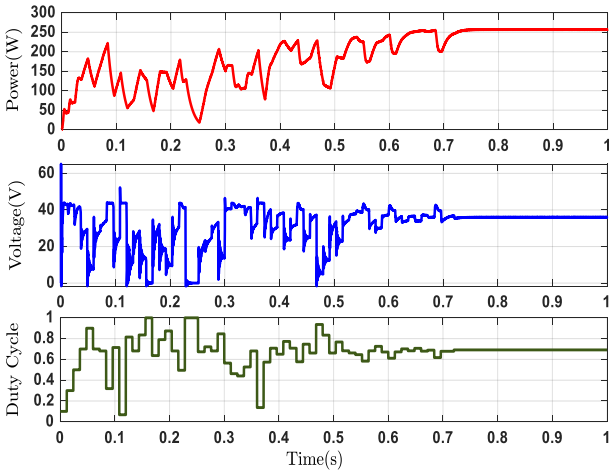


**(c) Classical GWO**

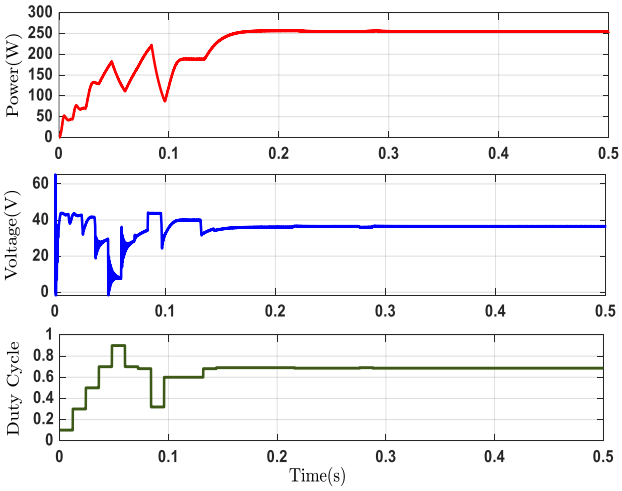


**(d) Modified GWO**

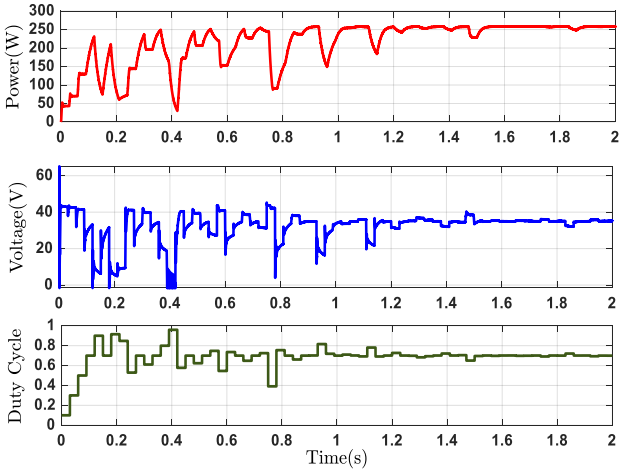


**(e) Classical PSO**

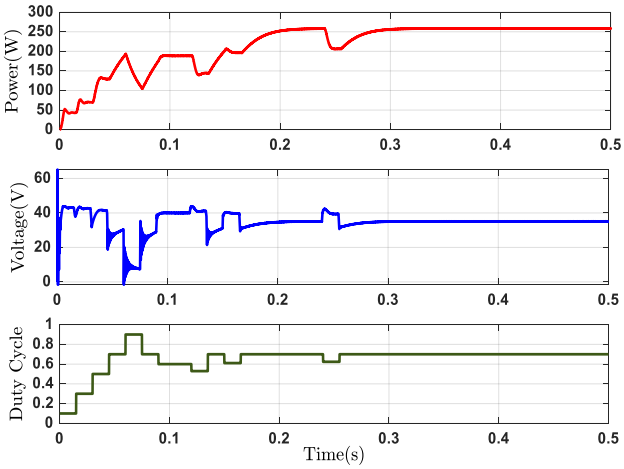


**(f) Modified PSO**

**Figure 12.** The PV Output Waveform for Pattern-1 by using different strategies (a) CCSA, (b) MCSA, (c) CGWO, (d) MGWO, (e) CPSO, (f) MPSO.

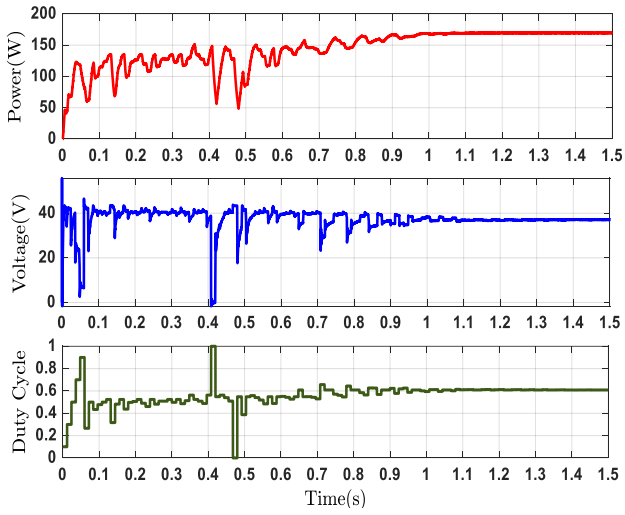


**(a) Classical CSA**

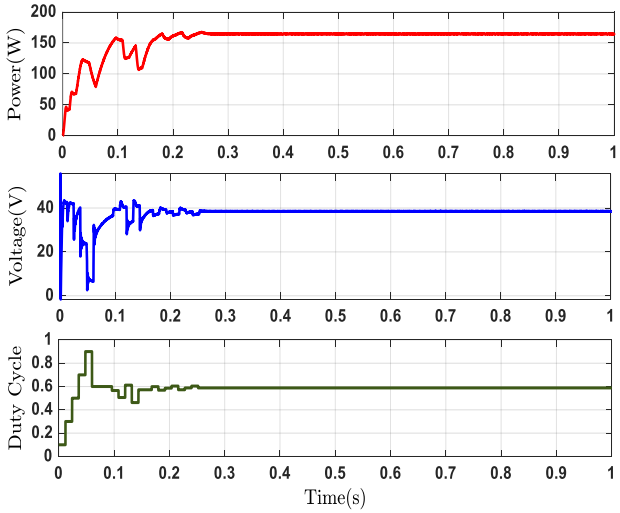


**(b) Modified CSA**

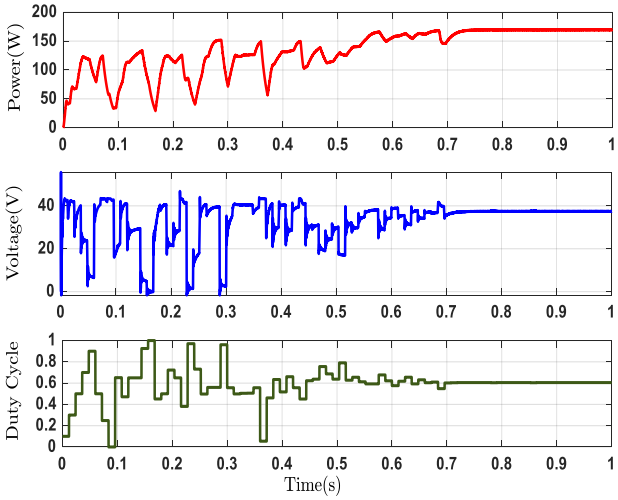


**(c) Classical GWO**

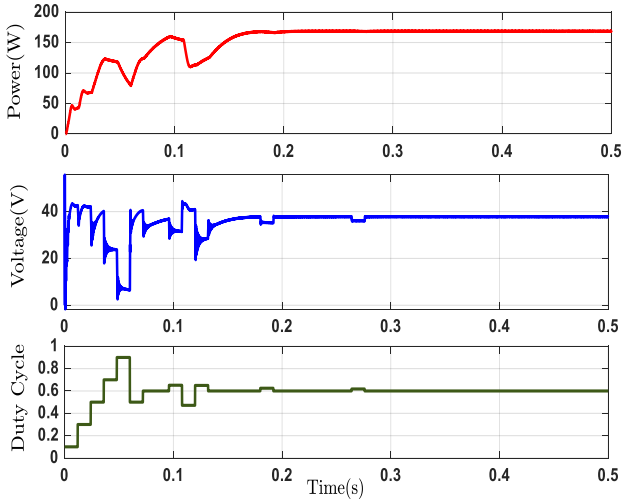


**(d) Modified GWO**

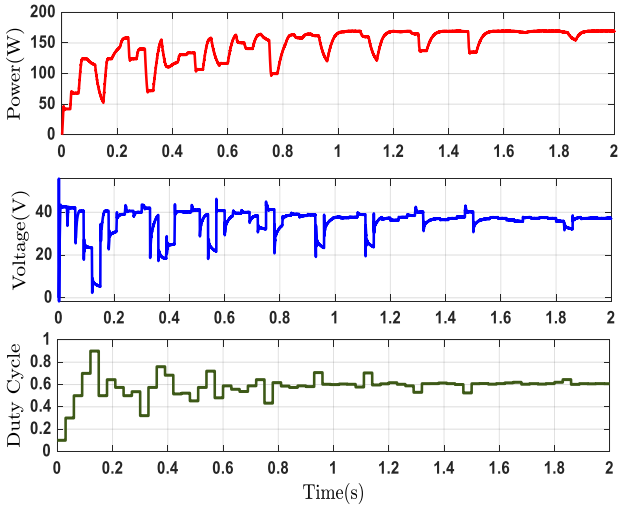


**(e) Classical PSO**

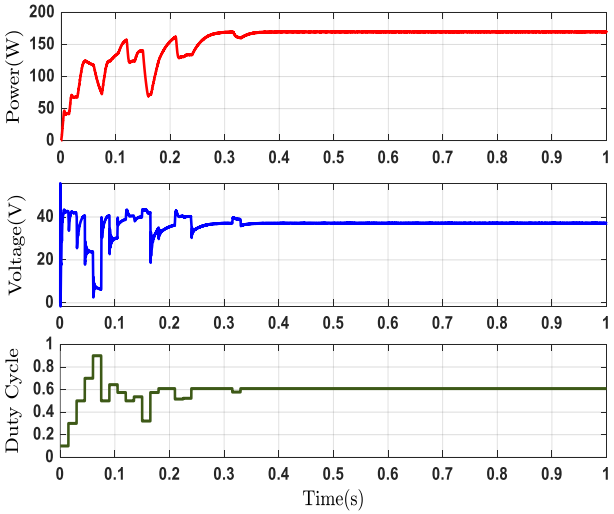


**(f) Modified PSO**

**Figure 13.** The PV Output Waveform for Pattern-2 by using different strategies (a) CCSA, (b) MCSA, (c) CGWO, (d) MGWO, (e) CPSO, (f) MPSO.

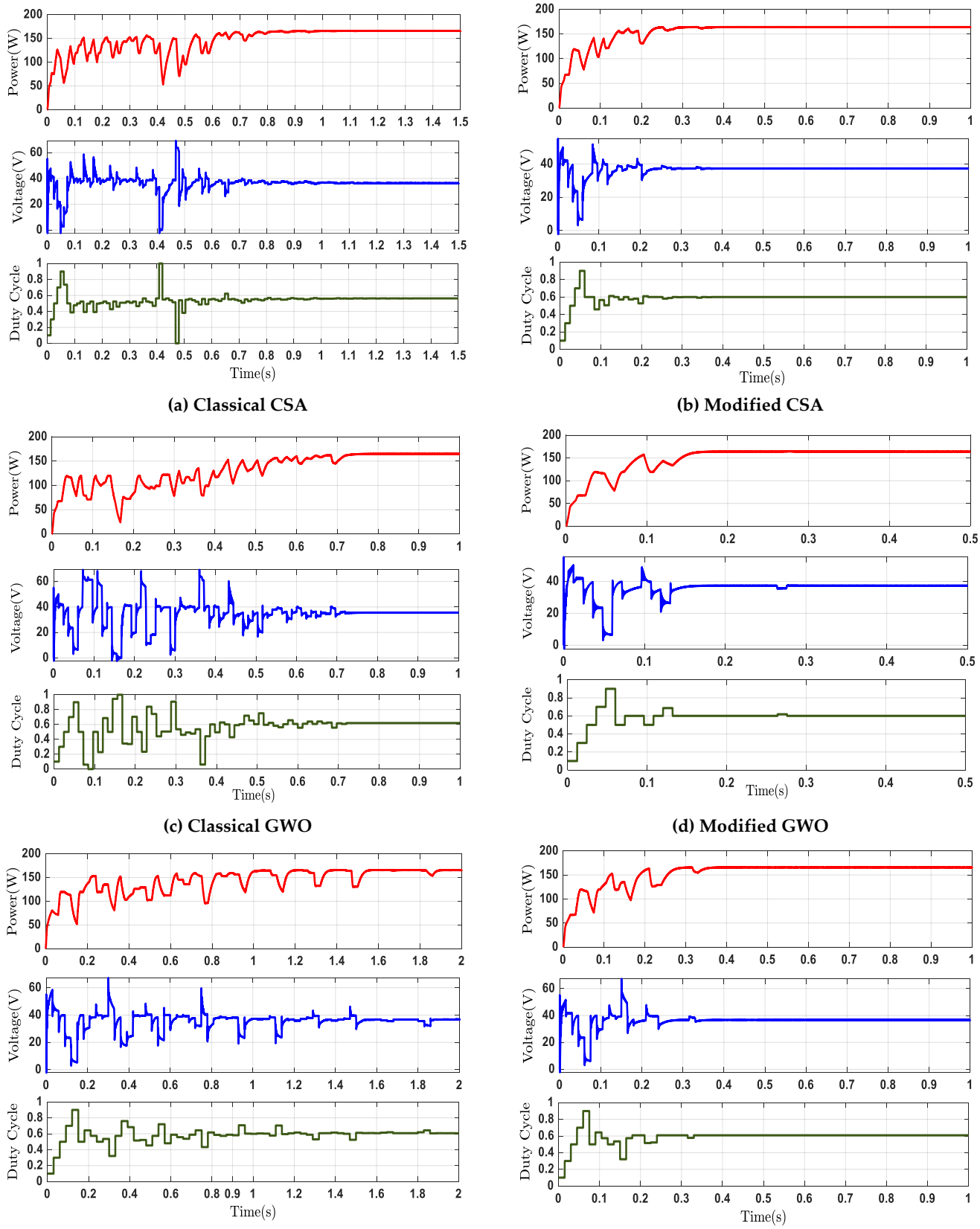


(a) Classical CSA

(b) Modified CSA

(c) Classical GWO

(d) Modified GWO

(e) Classical PSO

(f) Modified PSO

**Figure 14.** The PV Output Waveform for Pattern-3 by using different strategies (a) CCSA, (b) MCSA, (c) CGWO, (d) MGWO, (e) CPSO, (f) MPSO.

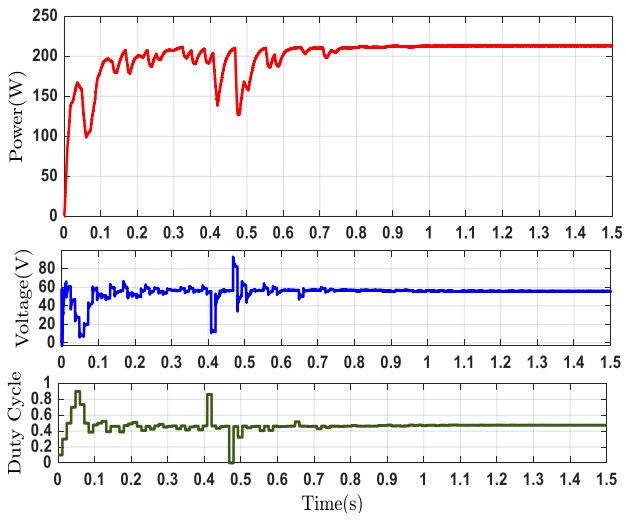


**(a) Classical CSA**

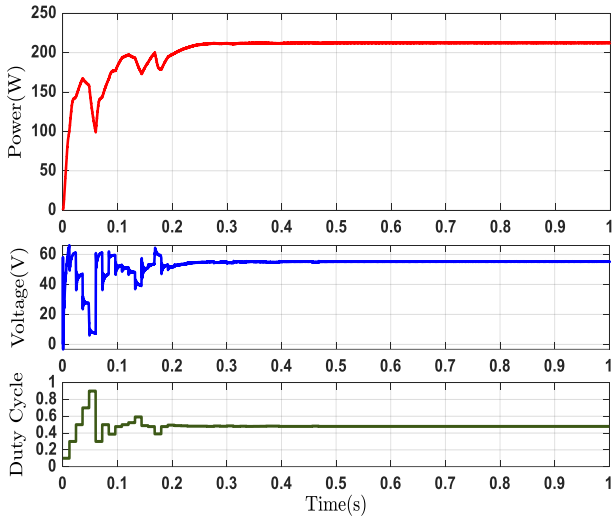


**(b) Modified CSA**

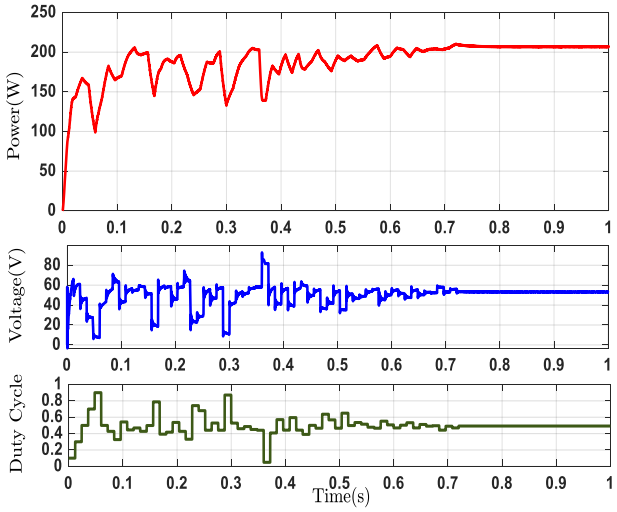


**(c) Classical GWO**

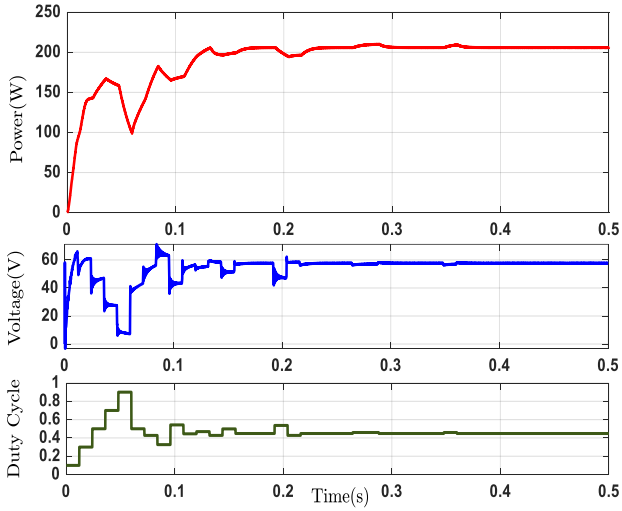


**(d) Modified GWO**

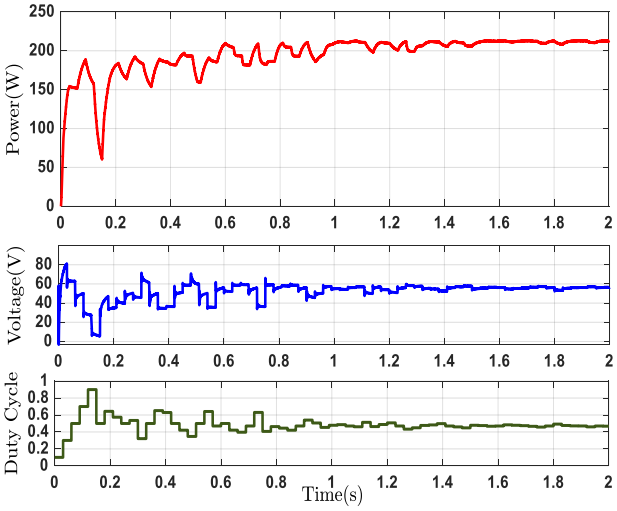


**(e) Classical PSO**

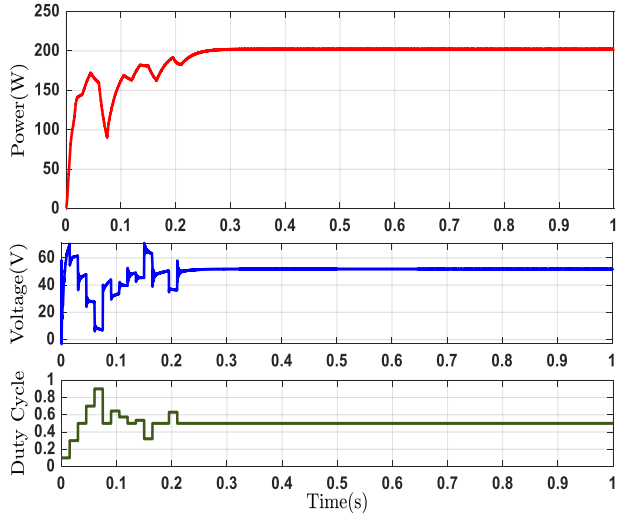


**(f) Modified PSO**

**Figure 15.** The PV Output Waveform for Pattern-4 by using different strategies (a) CCSA, (b) MCSA, (c) CGWO, (d) MGWO, (e) CPSO, (f) MPSO.

*3.6. Comparative Analysis for the Previous Evaluations*

By the previous evaluations, all the results can be summarizing at Table 2. Also, a comparative analysis for the classical and modified CSA, GWO, and PSO algorithms performance can be achieved. This comparison helps on choosing the effective controller strategy for letting the PV system dealing with the complex ISC.

**Table 2.** The PV Patterns Evaluations Results.

| Conditions | Algorithm | Output Power (W) | Efficiency | Convergence Speed (Sec) | Oscillation specification | |
|---|---|---|---|---|---|---|
| | | | | | Transient | Steady State |
| Normal Condition (No Shading) MPP is 260W at 35.5V | CSA | 254.2 | 97.77% | 0.8 | Medium Oscillations | High Stable |
| | GWO | 254.9 | 98.04% | 0.74 | High Oscillations | High Stable |
| | PSO | 254.7 | 97.96% | 1.53 | High Oscillations | Minor Oscillations |
| | MCSA | 254.1 | 97.73% | 0.49 | Slight Oscillations | High Stable |
| | MGWO | 257.6 | 99.08% | 0.17 | Slight Oscillations | High Stable |
| | MPSO | 257.1 | 98.88% | 0.29 | Slight Oscillations | High Stable |
| Irregular Shading (String of 2 PV Modules) GMPP is 170W at 37V | CSA | 168.27 | 98.98% | 0.98 | Medium Oscillations | High Stable |
| | GWO | 168.67 | 99.22% | 0.73 | High Oscillations | High Stable |
| | PSO | 168.2 | 98.94% | 1.89 | Medium Oscillations | Minor Oscillations |
| | MCSA | 166.68 | 98.05% | 0.25 | Slight Oscillations | High Stable |
| | MGWO | 168.6 | 99.18% | 0.17 | Slight Oscillations | High Stable |
| | MPSO | 168.53 | 99.14% | 0.35 | Slight Oscillations | High Stable |
| Complex Irregular Shading (String of 3 PV Modules) GMPP is 165W at 36.5V | CSA | 163.34 | 98.99% | 0.79 | Medium Oscillations | High Stable |
| | GWO | 164.49 | 99.69% | 0.73 | Medium Oscillations | High Stable |
| | PSO | 163.87 | 99.32% | 1.88 | Medium Oscillations | Minor Oscillations |
| | MCSA | 163.9 | 99.33% | 0.28 | Slight Oscillations | High Stable |
| | MGWO | 164.8 | 99.88% | 0.15 | Slight Oscillations | High Stable |
| | MPSO | 164.6 | 99.76% | 0.35 | Slight Oscillations | High Stable |
| More Complex Irregular Shading (String of 4 PV Modules) GMPP is 215W at 56V | CSA | 207.1 | 96.33% | 0.74 | Medium Oscillations | High Stable |
| | GWO | 210.26 | 97.80% | 0.72 | Medium Oscillations | High Stable |
| | PSO | 209.1 | 97.26% | 1.52 | Medium Oscillations | Minor Oscillations |
| | MCSA | 205.8 | 95.72% | 0.25 | Slight Oscillations | High Stable |
| | MGWO | 210.19 | 97.76% | 0.23 | Slight Oscillations | High Stable |
| | MPSO | 202.37 | 94.13% | 0.26 | Slight Oscillations | High Stable |

Firstly, the patterns' convergence speed results indicate that each modified algorithm outperforms its classic counterpart. It achieved the goal of tracking effectively in terms of tracking speed with minor oscillations. For instance, notable enhancements were achieved through the implementation of the modified PSO algorithm. The CPSO exhibited relatively prolonged stabilization times of 1.53s, 1.89s, 1.88s, and 1.52s. In comparison, the Modified PSO (MPSO) demonstrated significantly faster convergence, requiring only 0.29s, 0.35s, 0.35s, and 0.26s, respectively.

Secondly, it is observed that the tracking efficiency of all the modified algorithms is nearly equal. Therefore, the comparison criteria have been prioritized in order of significance: purposeful convergence speed, followed by lower oscillation during the transient state, and finally, tracking efficiency.

Thirdly, it is observed that the Modified Particle Swarm Optimization (MPSO) algorithm exhibits inferior performance compared to the other two algorithms, as it consistently records the longest convergence times across all evaluations of PV string operations under ISC.

Finally, the comparative analysis between the two most effective modified algorithms, MCSA and MGWO, results in selecting the optimal PV string controller strategy. The MGWO algorithm displays outstanding performance across all evaluations, particularly as the complexity of ISC increases. In the first evaluation, the MGWO algorithm delivered a higher efficiency of 99.08% at 0.17s. While the MCSA delivered 97.73% after 0.49s. In the second evaluation, the MGWO algorithm achieved a higher efficiency of 99.18% within 0.17s, whereas the MCSA achieved 98.05% after 0.25s. During the third evaluation, the MGWO algorithm attained a superior efficiency of 99.88% in just 0.15s, while the MCSA algorithm reached an efficiency of 99.33% after 0.28s. In the final evaluation, the MGWO algorithm demonstrated a higher efficiency of 97.76% within 0.23s, compared to the MCSA algorithm, which achieved 95.72% after 0.25s.

The superiority of the MGWO algorithm's performance over MCSA is due to two factors. The first factor is the dynamic design of the GWO algorithm, which depends on the effective balance of exploration and exploitation phases. It can be achieved by the individuals' organization of the GWO algorithm among three levels of searching ($\alpha$, $\beta$, $\delta$) to reach the best solution. The second factor is the effective modification that has been added to the GWO algorithm. It maintains a deliberate exploration of the search space, allowing the search to be quickly directed toward optimal solutions. Figures 13 and 14 are bar charts that were constructed to portray the algorithms' effective performance easily.

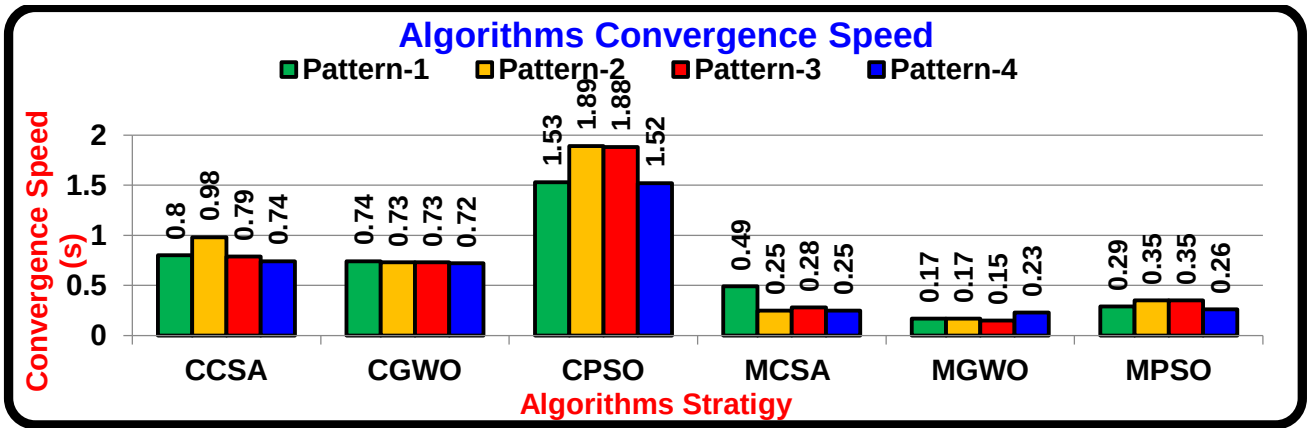


**Figure 16.** The Comparison Between Different Strategies Convergence Speed.

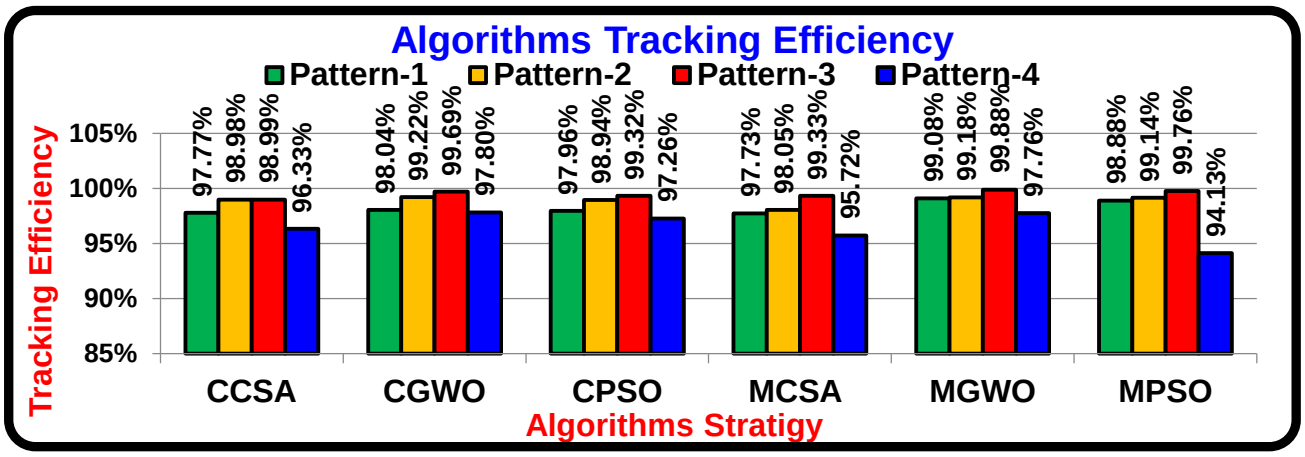


**Figure 17.** The Comparison Between Different Strategies Tracking Efficiency.

*3.7. Testing PV Water Pumps as an Application*

Solar water pumps are one of the most famous applications of PV panels in ISC. They operate in remote areas without electricity networks and are surrounded by irregular shading caused by trees, various plants, birds, and other factors.

In this tested application, the PV water pumping system consists of four parts, namely: the PV system, the DC to AC inverter, the Induction Motor, and the water pump as shown in Figure 18. The PV system has two PV strings associated with a DC-DC boost converter and controlled by one of the mentioned algorithm strategies (CCSA, CGWO, CPSO, MCSA, MGWO, MPSO) to track the global available output power. The inverter used to convert the DC-DC boost converter output DC voltage to AC voltage, which is suitable for driving the Induction Motor. The induction motor is more effective in this application for driving the water pump.

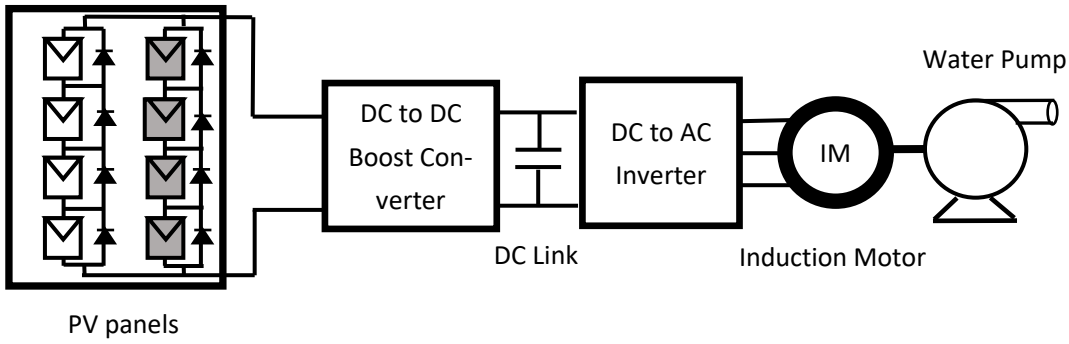


**Figure 18.** The PV Water Pumps as an Application.

The MATLAB / Simulink has been used to simulate that application to evaluate the solar water pumping system performance at different controller strategies. The PV panel was affected by ISC due to one of the surrounding factors. according to that, the first PV string received 1000 W/m^2, while the second PV string received 200 W/m^2. This condition lets the PV system's output power have a global maximum power of 915W and a local maximum power of 363W. The induction motor has the parameters of rated speed of 1420 rpm, rated voltage of 230V, and the nominal power of 1500W.

The simulation test results have been summarized in Table 3. These results stressed that the (MGWO) has the perfect performance for driving the PV water pump system. It extracts the higher power value of 912W from the PV system compared to the other algorithms, as shown in Figure 19 (d). It ended its tracking process during 0.025s. The induction motor rotor reached 698.7 rpm with a load torque of 2.59 N.m. The MCSA comes in the second arrangement for the system performance. It reached the global maximum power of 909W at 0.032s. In this case, the induction motor reached 697 rpm with a load torque of 2.54 N.m. The lowest performance is associated with the MPSO. It lets the induction motor reach 696 rpm when the algorithm extracts the power of 907W at 0.036s.

**Table 3.** The PV Water Pumping System Results.

| Algorithm | The PV System | | | | | The Water Pump | |
|---|---|---|---|---|---|---|---|
| | Output Power (W) | Efficiency | Convergence Speed (Sec) | Oscillation Specification | | Speed (rpm) | Torque (N.m) |
| | | | | Transient | Steady State | | |
| CCSA | 821 | 89.73% | 0.098 | High Oscillations | High Stable | 632 | 1.99 |
| CGWO | 881 | 96.28% | 0.025 | Slight Oscillations | High Stable | 672 | 2.23 |
| CPSO | 719 | 78.58% | 0.164 | Medium Oscillations | Minor Oscillations | 556.6 | 1.71 |
| MCSA | 909 | 99.34% | 0.032 | Slight Oscillations | High Stable | 697.3 | 2.54 |
| MGWO | 912 | 99.67% | 0.025 | Slight Oscillations | High Stable | 698.7 | 2.59 |
| MPSO | 907 | 99.13% | 0.036 | Slight Oscillations | High Stable | 696.2 | 2.5 |

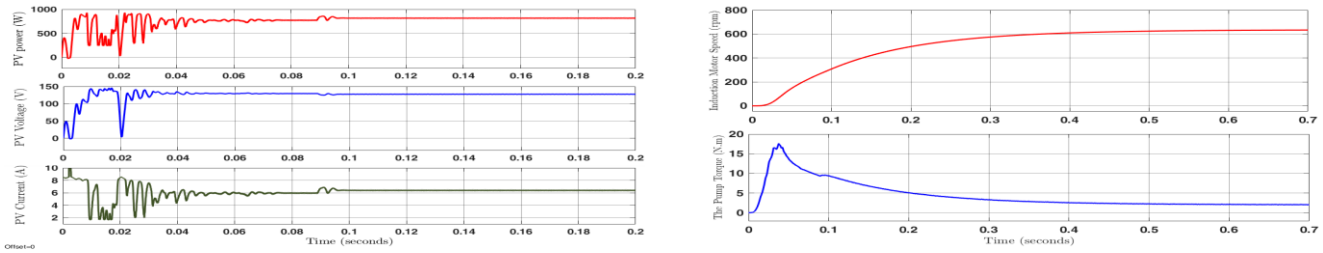


**(a) Classical CSA**

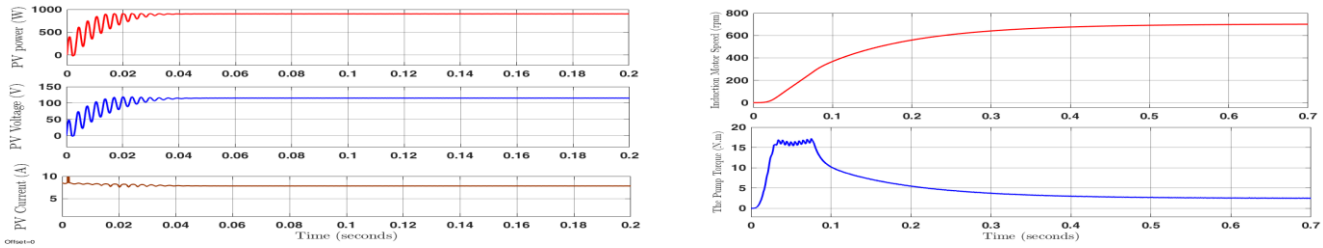


**(b) Modified CSA**

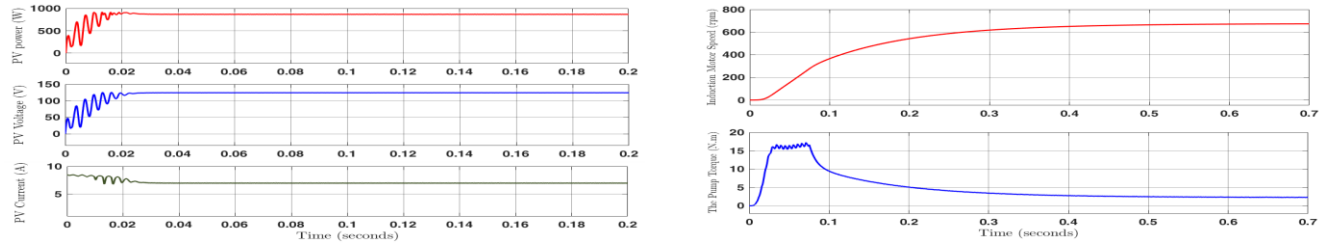


**(c) Classical GWO**

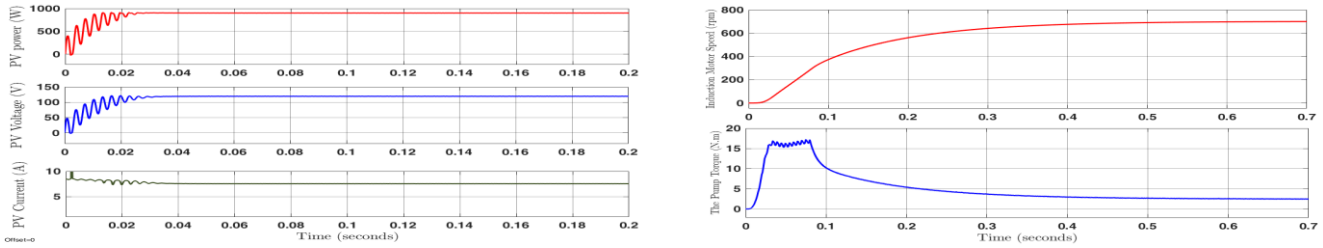


**(d) Modified GWO**

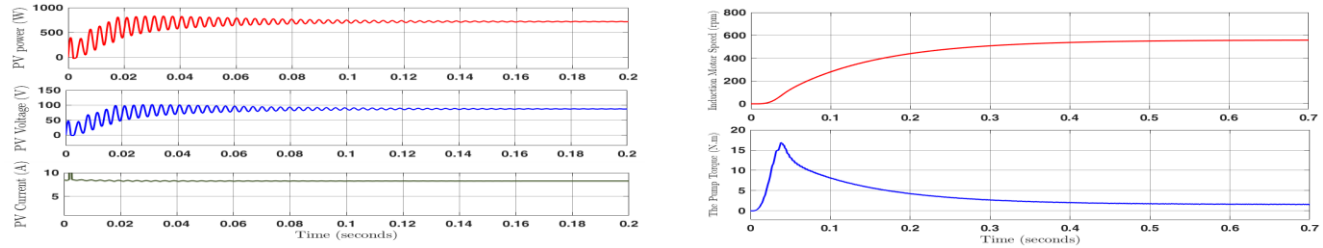


**(e) Classical PSO**

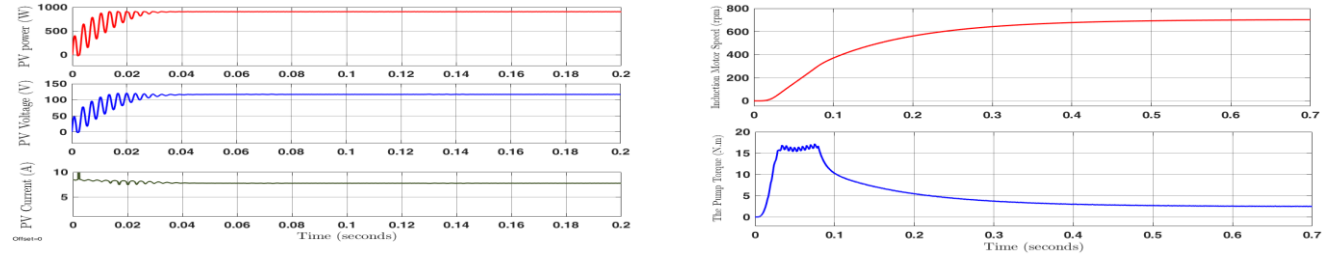


**(f) Modified PSO**

**Figure 19.** The PV Outputs, the Induction Motor Speed (rpm), and the Pump torque Waveforms for the PV Water Pumping System using different strategies (a) CCSA, (b) MCSA, (c) CGWO, (d) MGWO, (e) CPSO, (f) MPSO.

Figures 17 and 18 are bar charts that were constructed to portray the algorithms' effective performance for the PV Water Pump application easily.

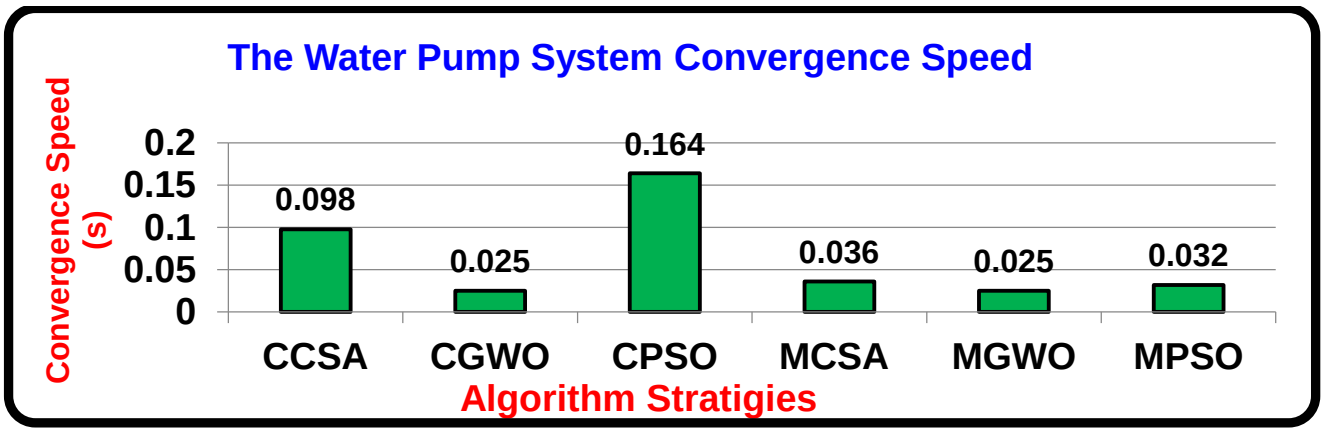


**Figure 20.** The Comparison Between Different Strategies Convergence Speed for PV Water Pump as an Application.

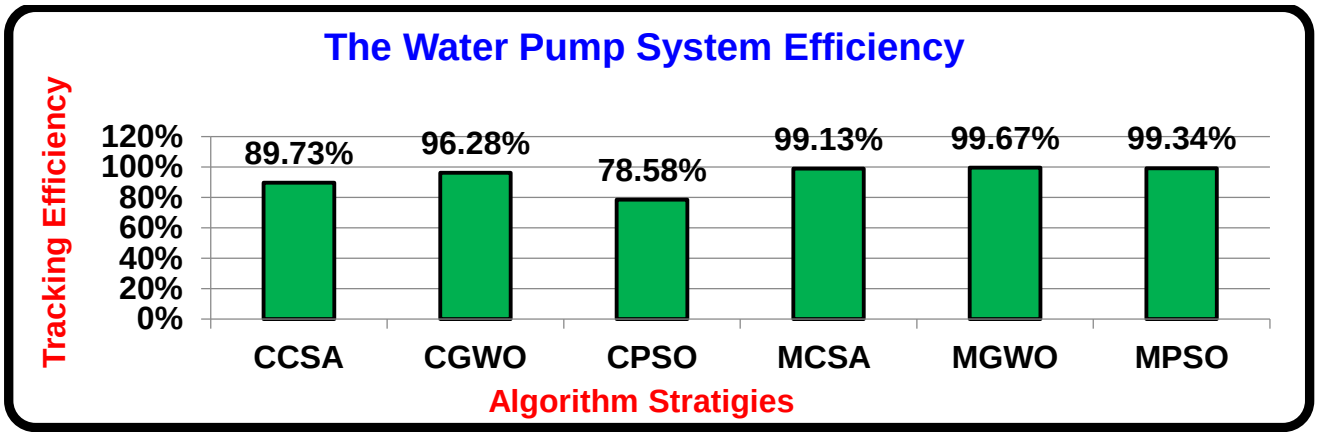


**Figure 21.** The Comparison Between Different Strategies System Efficiency for PV Water Pump as an Application.

## 4. The Experimental Results

The performance of the proposed modified algorithms was experimentally validated through a laboratory test, as illustrated in Figure 22(a). The experimental setup comprises three primary components. The first component is the PV emulator, implemented using two adjustable DC power supplies in conjunction with multiple power resistors to simulate various irradiation conditions. The second component is the power interface, which consists of a boost converter equipped with a 3 mH, 7 A inductor, a capacitor bank rated at 2×2200 μF/50 V, a 100 V/10 A fast recovery diode, and a 100 V/25 A power MOSFET. The third component is the control unit, which includes a voltage sensor, a current sensor, a gate driver, and a TMS320F28335 digital signal controller (32-bit, 150 MHz). The output of the system is connected to a battery bank composed of two 12 V, 7 Ah batteries.

In this experimental case study, the two DC power supplies are configured to output 20 V, and two power resistors with values of 4.4 Ω and 1.5 Ω are employed, as illustrated in Figure 22(b). This configuration emulates a partially shaded PV scenario, resulting in two distinct maximum power points (MPPs) at 68.9 W and 61 W as shown in Figures 22 (c). To evaluate the tracking capability under such conditions, the standard GWO and its modified version MGWO are selected for performance comparison.

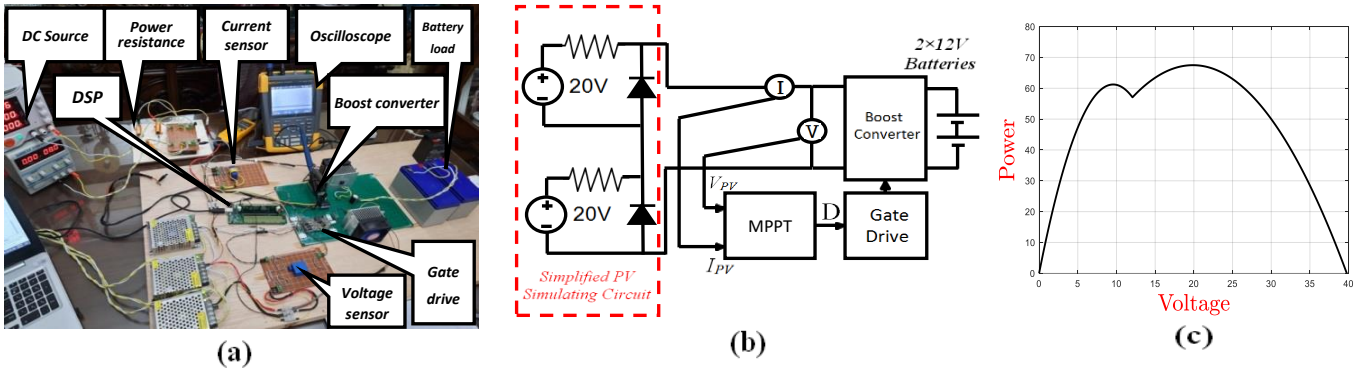


**Figure 22.** The experimental construction (a) The experimental photography (b) The schematic diagram (c) The P-V curve of simulated PV circuit.

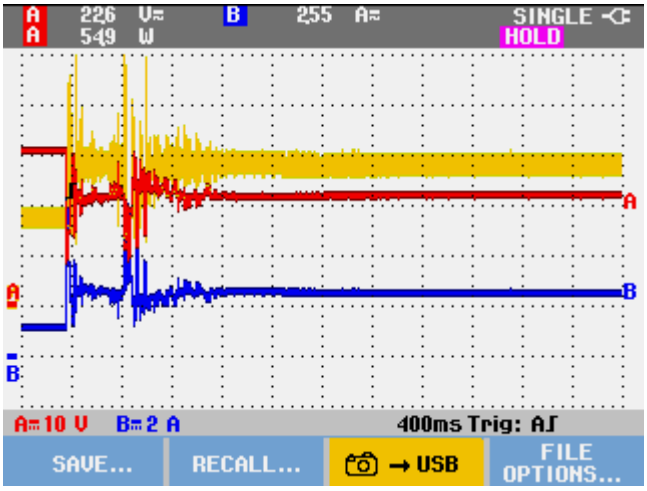


**(a) Classical GWO**

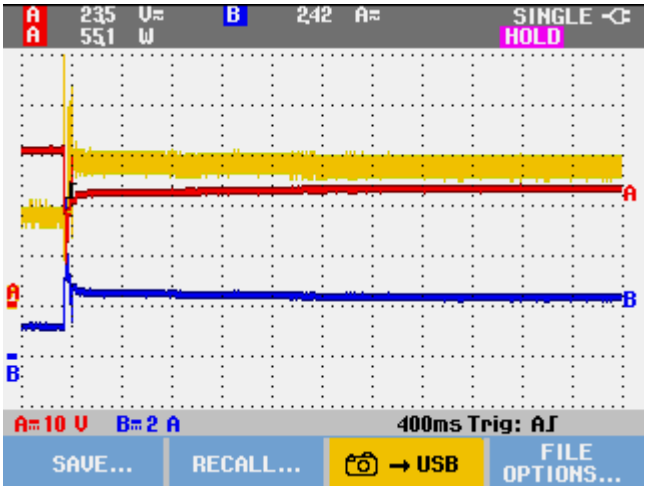


**(b) Modified GWO**

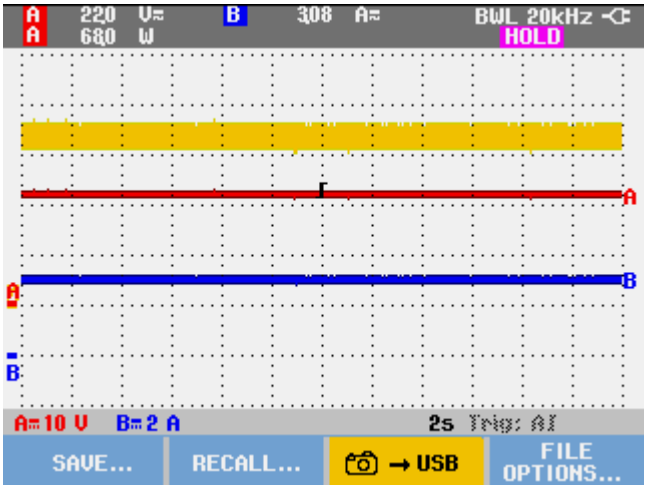


**(c) Classical GWO**

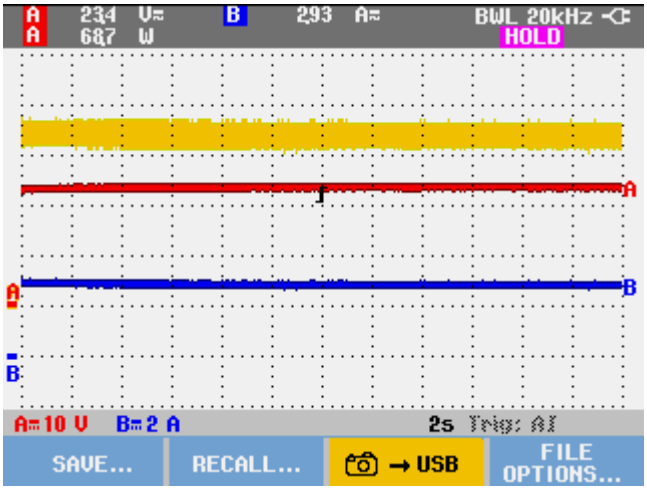


**(d) Modified GWO**

**Figure 23.** The convergence waveform in the practical experiment under irregular shading conditions, (a) the transient waveform of the Classical GWO method, (b) the transient waveform of the Modified GWO method, (c) the steady state waveform of the Classical GWO method, (d) the steady state waveform of the Modified GWO method

The classical GWO algorithm required approximately 1.2s to converge and locate the global maximum power point GMPP, as depicted in Figure 23 (a). It subsequently stabilized at an GMPP of 68 W under steady-state conditions, corresponding to an operating voltage of 22 V and a current of 3.08 A, as shown in Figure 23 (c). In contrast, the MGWO demonstrated significantly faster convergence, reaching the GMPP in about 0.24s, as presented in Figure 23 (b). Following convergence, it delivered approximately 68.7 W to the load with enhanced power stability, maintaining an operating voltage of 23.4 V and a current of 2.93 A, as illustrated in Figure 23 (d).

These experimental results highlight the superior performance of the MGWO algorithm, which achieved a practical efficiency of 99.56%, demonstrating faster tracking speed and improved steady-state stability. Meanwhile, the classical GWO yielded a lower efficiency of 98.55%, with slower convergence and less stable power output during steady-state operation.

## 5. Conclusions

Choosing a high-performance and more effective strategy for the PV system controller to extract the maximum available power is very significant during the design process. This study presented a comparative analysis of three powerful algorithms in their classical and modified form to choose the highest-performing one. These algorithms are the Cuckoo Search Algorithm (CSA), the Grey Wolf Optimization (GWO) algorithm, the Particle Swarm Optimization (PSO) algorithm, the Modified Cuckoo Search Algorithm (MCSA), the Modified Grey Wolf Optimization (MGWO), and the Modified Particle Swarm Optimization (MPSO). The comparison was conducted by progressively increasing the complexity of irregular shading on the PV panels to evaluate the algorithm's effectiveness in handling such challenging conditions. The results indicate that the classical GWO algorithm has the highest performance compared to the other two classical algorithms due to its effective balance between exploration and exploitation. It has a social hierarchy, and the hunting behavior of grey wolves (GWO) enables a more structured and adaptive search process. Unlike the PSO algorithm, which can suffer from premature convergence and reduced diversity in later stages. Similarly, although CSA utilizes Lévy flights to enhance exploration, it lacks the structured convergence exhibited by GWO, which is driven by the collaborative guidance of the alpha, beta, and delta wolves.

By adding a powerful technique to the classical versions, the modified algorithms consistently outperformed the conventional counterparts by effectively minimizing oscillations in PV output power, achieving faster convergence to the maximum available power, and enhancing overall tracking efficiency. Among the evaluated techniques, the Modified Grey Wolf Optimizer (MGWO) exhibited the best performance, followed by the Modified Cuckoo Search Algorithm (MCSA), while the Modified Particle Swarm Optimization (MPSO) showed the least favorable results, as indicated by key performance metrics.

Furthermore, the algorithms were validated in a simulated application involving water pumping using an induction motor by using a MATLAB / Simulink program. The results confirmed that the Modified Grey Wolf Optimization (MGWO) algorithm led to superior motor performance, characterized by higher rotational speed and torque response, compared to the other algorithms. The findings advocate for the use of the Modified Grey Wolf Optimization (MGWO) algorithm to enhance PV's system reliability, power generation, and operational stability in renewable energy applications.

## References

1. Guanghua, L., Siddiqui, F. A., Aman, M. M., Shah, S. H. H., Ali, A., Soomar, A. M., & Shaikh, S. (2024). Improved maximum power point tracking algorithms by using numerical analysis techniques for photovoltaic systems. Results in engineering, 21, 101740.
2. Ballouti, A., Chouiekh, M., Ameziane, H., El Mourabit, Y., & Zakriti, A. (2024, June). Enhancing photovoltaic performance using artificial intelligence methods based on Fuzzy Logic. In 2024 16th International Conference on Electronics, Computers and Artificial Intelligence (ECAI) (pp. 1-4). IEEE.
3. Kamal, R., Abdel-Salam, M., & Nayel, M. (2024). Maximum power point tracking in PV arrays exposed to partial shading condition irrespective of the array configuration. Energy Systems, 1-40.
4. Abdulhadi, H. M. (2025). Improved DC-DC converter based on quadruple boosting technique for high-voltage gain in photovoltaic systems. Electrical Engineering, 107(4), 5231-5246.
5. Gil-Velasco, A., & Aguilar-Castillo, C. (2021). A modification of the perturb and observe method to improve the energy harvesting of PV systems under partial shading conditions. Energies, 14(9), 2521.

6. de Oliveira, F. M., Brandt, M. H. M., Salvadori, F., Izquierdo, J. E. E., Cavallari, M. R., & Ando Junior, O. H. (2024). Development of an MPPT-based genetic algorithm for photovoltaic systems versus classical MPPT techniques in scenarios with partial shading. Inventions, 9(3), 64.
7. Chtita, S., Motahhir, S., El Hammoumi, A., Chouder, A., Benyoucef, A. S., El Ghzizal, A., ... & Askar, S. S. (2022). A novel hybrid GWO–PSO-based maximum power point tracking for photovoltaic systems operating under partial shading conditions. Scientific Reports, 12(1), 10637.
8. Mathi, D. K., & Chinthamalla, R. (2020). A hybrid global maximum power point tracking method based on butterfly particle swarm optimization and perturb and observe algorithms for a photovoltaic system under partially shaded conditions. International Transactions on Electrical Energy Systems, 30(10), e12543.
9. Kumar, S. S., & Balakrishna, K. (2024). A novel design and analysis of hybrid fuzzy logic MPPT controller for solar PV system under partial shading conditions. Scientific Reports, 14(1), 10256.
10. [10] Zafar, M. H., Khan, N. M., Mirza, A. F., Mansoor, M., Akhtar, N., Qadir, M. U., ... & Moosavi, S. K. R. (2021). A novel meta-heuristic optimization algorithm based MPPT control technique for PV systems under complex partial shading conditions. Sustainable Energy Technologies and Assessments, 47, 101367.
11. Ali, Ehab Mohamed; Hossam-Eldin, Ahmed A.; Abdelsalam, Ahmed K. An Enhanced Particle Swarm Optimization Algorithm Fitting for Photovoltaic Max Power Tracking under Different Climatic Conditions. In: 2021 International Telecommunications Conference (ITC-Egypt). IEEE, 2021. p. 1-4.
12. Ali, Ehab Mohamed; Mohamed, Wael Mokhtar. A Powerful Technique Associated with Grey Wolves Optimization Algorithm to Track the PV Modules' Global Maximum Power During Partial Shading. In: 2024 International Telecommunications Conference (ITC-Egypt). IEEE, 2024. p. 1-6.
13. Hossam-Eldin, Ahmed A., et al. Fast Convergence Modified Cuckoo Search Algorithm to Pursue String PV Modules Maximum Power Point under Partial Shading Conditions. In: 2020 30th International Conference on Computer Theory and Applications (ICCTA). IEEE, 2020. p. 101-107.
14. Ali, E. M., Mokhtar, W. M., & Fiyad, H. M. N. (2023, July). An Effective Strategy Coupled with Perturb and Observe Algorithm to Track the PV Systems' Global Maximum Power under Partial Shading Conditions. In 2023 International Telecommunications Conference (ITC-Egypt) (pp. 692-695). IEEE.
15. Khalid, M., Murtaza, S., Bano, M., Shafiq, I., & Jawaria, R. (2024). Role of extended end-capped acceptors in non-fullerene-based compounds towards photovoltaic properties. Journal of Photochemistry and Photobiology A: Chemistry, 448, 115292.
16. Ali, E. M., Abdelsalam, A. K., Youssef, K. H., & Hossam-Eldin, A. A. (2021). An enhanced cuckoo search algorithm fitting for photovoltaic systems' global maximum power point tracking under partial shading conditions. Energies, 14(21), 7210.
17. Tariq, M., Rihan, M., & Ayan, M. (2024). A comprehensive review on the application of recently introduced optimization techniques obtaining maximum power in the solar PV System. Renewable Energy Focus, 100564.
18. Abualigah, L., Ababneh, A., Ikotun, A. M., Zitar, R. A., Alsoud, A. R., Khodadadi, N., ... & Jia, H. (2024). A Survey of cuckoo search algorithm: optimizer and new applications. In Metaheuristic optimization algorithms (pp. 45-57). Morgan Kaufmann.
19. Bhattacharjee, A., & Mikkili, S. (2024, December). Cuckoo Search Based MPPT with Quadra Tied Solar PV Array for Maximizing Power Extraction Under Partial Shadows. In TENCON 2024-2024 IEEE Region 10 Conference (TENCON) (pp. 1333-1336). IEEE.
20. Nasir, M., Sadollah, A., Mirjalili, S., Mansouri, S. A., Safaraliev, M., & Rezaee Jordehi, A. (2024). A Comprehensive Review on Applications of Grey Wolf Optimizer in Energy Systems. Archives of Computational Methods in Engineering, 1-41.
21. Hadi, H. A., Kassem, A., Amoud, H., Nadweh, S., & Ghazaly, N. M. (2024). Using grey wolf optimization algorithm and whale optimization algorithm for optimal sizing of grid-connected bifacial PV systems. Journal of Robotics and Control (JRC), 5(3), 733-745.
22. Xu, S. Z., & Zhong, Y. M. (2024). NSNPSO-INC: A simplified particle swarm optimization algorithm for photovoltaic MPPT combining natural selection and conductivity incremental approach. IEEE Access.
23. Gupta, J., Beryozkina, S., Aljaidi, M., Singla, M. K., Safaraliev, M., Gupta, A., & Nijhawan, P. (2024). Application of hybrid chaotic particle swarm optimization and slime mould algorithm to optimally estimate the parameter of fuel cell and solar PV system. International Journal of Hydrogen Energy, 83, 1003-1023.
24. Ali, E. M., & Hossam Eldin, A. (2021). Fast Convergence Modified Particle Swarm Optimization Algorithm to Follow up String PV Modules Maximum Power Point under Different Climatic Conditions. International Journal of Telecommunications, 1(01), 1-16.